1-1-2016

An Experimental Investigation On The Effect Of Intake Charge Temperature And Injection Timing On Autoignition Of Low Cetane Number Fuel (sasol Ipk)

Swapnil Shekhar Bodele
Wayne State University,

AN EXPERIMENTAL INVESTIGATION ON THE EFFECT OF INTAKE CHARGE TEMPERATURE AND INJECTION TIMING ON AUTOIGNITION OF LOW CETANE NUMBER FUEL (SASOL IPK)

by

SWAPNIL S BODELE

THESIS

Submitted to the Graduate School

of Wayne State University,

Detroit, Michigan

in partial fulfillment of the requirements

for the degree of

MASTER OF SCIENCE

2016

MAJOR: MECHANICAL ENGINEERING

Approved by:

_____

Advisor Date

DEDICATION

I dedicate this work to my parents, professors, the auto sector and the evergreen PNGV engine...

ACKNOWLEDGMENTS

I would like to express my deepest gratitude and appreciation to my advisor Dr. Henein, who gave me this opportunity to work under his guidance in PNGV lab at the Center of Automotive Research at Wayne State University. His support, guidance, and vast ocean of knowledge at every step provided an unmatched learning experience throughout my graduate studies. His patience and enthusiasm taught me life lessons.

I am thankful to my committee members for their moral support and guidance.

Special thanks to the Center of Automotive Research, Wayne State University and US Army TARDEC for such advanced research facility.

I also thank all the talented CAR members, specially my lab mates, Krishnaraj and Manan for their help, support, guidance and never ending knowledge sharing sessions which provided new directions to research.

Heartfelt thanks to my knowledgeable seniors Dr. Joshi, Dr. Zheng and Dr. Shrestha for acquainting me with the engine and lab instrumentation. They have been source of motivation and inspiration throughout the research.

Technical support by Lidia, Marvin and Eugene and administrative support by Kayla and Rosalind are highly appreciated.

Last but not the least, I would like to thank my parents, brother and better half for their incomparable patience and support.

Swapnil S Bodele

March 2016, Detroit MI

TABLE OF CONTENTS

DEDICATION i

ACKNOWLEDGMENTS ii

TABLE OF CONTENTS iii

LIST OF TABLES viii

LIST OF FIGURES vii

CHAPTER 1 INTRODUCTION 1

CHAPTER 2 LITERATURE REVIEW 3

2.1 Autoignition Process and Ignition Delay Period 3

2.2 Physical Ignition Delay Period 4

2.3 Chemical Ignition Delay Period 8

2.4 Ignition Delay and Temperature effects on Ignition Delay 12

CHAPTER 3 EXPERIMENTAL SETUP 24

3.1 Engine Test Cell Setup 24

3.2 Engine Specification 26

3.3 Intake Air System 28

3.4 Engine Cooling System 29

3.5 Oil flow in the System 29

3.6 Fuel System 30

3.7 Data Acquisition System 32

3.8 Target Fuel 34

CHAPTER 4 IGNITION DELAY DEFINITIONS 35

CHAPTER 5 RESULTS..... 38

5.1. Effect of varying Intake Air Temperature (Constant SOI) 40

5.1.1. Effect of varying Intake Air Temperature on In-cylinder Pressure..... 42

5.1.2. Effect of varying Intake Air Temperature on In-cylinder Temperature. 43

5.1.3. Effect of varying Intake Air Temperature on Rate of Heat Release .. 45

5.1.4. Effect of varying Intake Air Temperature on NTC Regime and Cool Flame..... 47

5.1.5. Observations based on zoomed RHR graph 49

5.1.6. Ignition Delay Determination at varying intake air temperatures..... 49

5.2. Effect of varying SOI at constant Intake Air Temperature..... 52

5.2.1. Effect of varying SOI at Intake Air Temperature of 70°C on In-cylinder Pressure. 53

5.2.2. Effect of varying SOI at Intake Air Temperature of 70°C on In-cylinder Temperature. 54

5.2.3. Effect of varying SOI at Intake Air Temperature of 70°C on Rate of Heat Release. 55

5.2.4. Effect of varying SOI at Intake Air Temperature of 70°C on NTC regime..... 56

5.2.5. Observations based on zoomed RHR graph 56

5.2.6. Ignition Delay Determination at varying SOI 57

5.3. Activation Energy (Ea) calculations: 58

5.4. Discussions 60

CHAPTER 6 CONCLUSIONS AND RECOMMENDATIONS 63

6.1. Conclusions 63

6.2. Future Recommendations 64

APPENDIX A..... 65

APPENDIX B..... 66

REFERENCES..... 67

ABSTRACT 80

ABBRVIATIONS ……82

AUTOBIOGRAPHICAL STATEMENT ……...83

LIST OF TABLES

Table 2.1: Baseline Test Conditions [80] ……...21

Table 3.1: Table showing Engine Specifications [82] ……..27

Table 5.1: Data Points at different SOI and Inlet temperatures ……39

Table 5.2: Reduction in ID as an effect of T_{int} at SOI of -2, -4 and -6 CAD ……....46

Table 5.3: ID values ……..52

Table 5.4: ID values for SOI -2, -4 and -6 at constant T_{in} ……...58

Table 5.5: Calculations of E_a for CA_{RP} and CA5 SOC definitions ……....60

Table 5.6: P_{mean} and P_{SOI} values at different intake temperature for particular SOI.....61

LIST OF FIGURES

Figure 1.1: Oil import status of US [1] 1

Figure 2.1: Pressure traces for a blend of Hexadecane and HMN in air and nitrogen [56] 7

Figure 2.2: Schematic showing Hydrocarbon oxidation [61] 9

Figure 2.3. Different stages of auto ignition using Heat Release Rate [63] 11

Figure 2.4: Correlation between Ignition delay and T log P [68] 14

Figure 2.5: Effect of intake air temperature on ignition delay of different CN fuels [76] 16

Figure 2.6: Relative luminosity under different temperatures and densities [77] 17

Figure 2.7: Ignition Delay versus 1/temperature at ambient condition [79].....18

Figure 2.8: Ignition Delay versus 1/temperature at different conditions [79] 19

Figure 2.9: Liquid lengths of Diesel and JP-8 at different temperatures and charge densities. [79] 20

Figure 2.10: Characteristics parameters of Rate of Heat Release [80] 21

Figure 2.11: Effect of Intake temperature on Rate of Heat Release Parameter [80].....22

Figure 2.12: Effect of intake temperature and load on NTC regime [81] 23

Figure 3.1: Picture of PNGV test cell [82] 25

Figure 3.2: Schematic diagram of the complete experimental setup [82] 26

Figure 3.3: Schematic diagram showing Intake Air flow in the system [83] 28

Figure 3.4: Schematic diagram of the Engine cooling system [83] 29

Figure 3.5: Schematic diagram showing Oil flow in the system 30

Figure 3.6: Schematic diagram of Fuel delivery system 32

Figure 4.1: ID definitions comparison using CuRHR trace [83] 36

Figure 5.1: Comparison of pressure traces at SOI of -2, -4 and -6 CAD 40

Figure 5.2: Comparison of temperature traces at SOI of -2, -4 and -6 CAD 43

Figure 5.3: Effect of temperature on RHR traces at SOI of -2, -4 and -6 CAD 45

Figure 5.4: Effect of temperature on RHR (zoomed) traces at SOI -2, -4 and -6 CAD…….47

Figure 5.5.a : ID determination for SOI -2 with varying intake air temperature 50

Figure 5.5.b : ID determination for SOI -4 with varying intake air temperature 51

Figure 5.5.c : ID determination for SOI -6 with varying intake air temperature 51

Figure 5.6: Pressure traces at constant T_{int} of 70°C and varying SOI of -2, -4, -6 53

Figure 5.7: Temperature traces at constant T_{int} of 70°C and varying SOI of -2, -4, -6 CAD 54

Figure 5.8: RHR traces at constant T_{int} of 70°C and varying SOI of -2, -4, -6 CAD 55

Figure 5.9: Zoomed RHR traces at constant T_{int} of 70°C and varying SOI of -2, -4, -6 CAD.....56

Figure 5.10: ID determination for SOI -2, -4, -6 at constant intake air temperature……57

Figure 5.11: Arrhenius plots of ID v/s 1/T for CA_{RP} and CA5 59

CHAPTER 1

INTRODUCTION

Diesel engines are always known for their efficiency and heavy-duty working capabilities. Engines invented to suffice stationary applications back in 1893 have become one of the major powerhouses for supply chain industry. Most of the cargo transportation in US is dependent on the diesel engines. Upsurge in oil demands resulted in inflation of its imports from other sources.

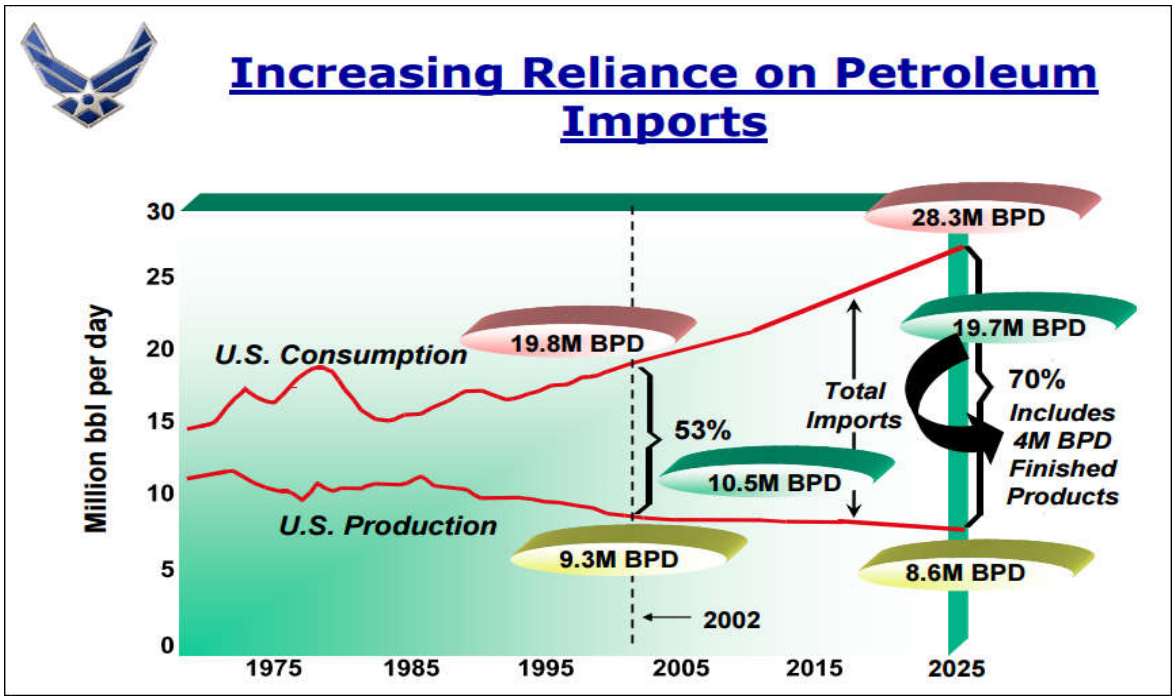

Figure 1.1: Oil import status of US [1]

Figure 1.1 shows the current and projected oil imports in US according to a study conducted by Air Force Research laboratory, AFB Ohio. Oil, specifically diesel, plays a crucial role in defense industry because of the use of heavy-duty engines.

Considering extensive use of aviation fuels in defense sector, logistics and transportation issues are moderated using “Single Fuel Concept” [2]. In March 1988, Department Of Defense adopted jet fuel JP8 as an alternative fuel to diesel under Single Fuel Concept. JP8 with high derived cetane number (DCN: 50.1) and better combustion characteristics at low temperature operates suitably at all conditions. However, due to increased rate of depletion in oil from petroleum resources, efforts are taken to blend and test the combustion and emissions characteristics JP8 with alternatives fuels prepared from other sources.

One such fuel, Iso Paraffinic Kerosene, a synthetic fuel developed by SASOL Company using Fischer-Tropsch [1] method is considered a good blend and several research are being conducted on the compatibility of that fuel to improve the overall performance and emission efficiency of diesel engines without making major changes to present engines.

Center of Automotive Research (CAR, Wayne State University) has been at par in conducting research on SASOL IPK. This experimental investigation is an extension of the studies carried out previously on similar kind of fuels but with different cetane numbers, which results in variations in autoignition, combustion and emission characteristics. This report focuses on effects of intake charge temperature and injection timing on autoignition of SASOL IPK (DCN: 31.17)

CHAPTER 2

LITERATURE REVIEW

Since the invention of combustion engines Diesel engines always showed higher efficiency of about 55% [3,4,5] at low speeds and about 45% at high speeds with lower CO and HC emissions but have high limitations in soot and NOx emissions [6-12] as compared to 40% efficiency of gasoline engines. To produce cleaner diesel engines consistent efforts are taken on both engine modification like development of common rail injection systems [13-15] as well as developing cleaner fuels like reducing low Sulphur content diesel and developing alternative fuels. Alternative fuels includes renewable fuels like bio-diesel [16-19] and ethanol [20-24] and non-renewable synthetic fuels like S-8 [25, 26] and Sasol IPK [27-29]. Synthetic fuels are manufactured by a process called Fisher-Tropsch process [95-100] and divided into two main groups Coal-to-Gas[103-105] and Coal-to-Liquid [30-31, 101,102]. Therefore, as the sources of fuel differ they show significant differences in their physical and chemical ignition delays.

2.1 Autoignition Process and Ignition Delay Period

Autoignition process is referred to a phenomenon which leads to combustion of diesel fuel taking into account the physical process which helps in formation of combustible mixture and chemical process which is responsible for all the reactions that starts combustion. In diesel engines, autoignition process is controlled mainly by chemical reactions than physical process [32]. To improve engine performance, fuel

economy and to reduce emissions, a good understanding of autoignition process is necessary [33, 34-37].

Dixon et al [38] first discovered in 1914 that when a combustible fuel–air mixture is burned in a glass cylinder, it burns after some delay of time, which is referred to as Ignition Delay. It was in 1920 when for the first time Hawk [39] experimentally measured the ignition delay time in diesel engine. However, the results from Dixon and Hawk were differing, showing significant physical ignition delay time in diesel engine. Initially even other researchers like Otto, Neuman and Sass [40-42] denied existence of physical ignition delay in diesel engines until works of Tausz and Schulte [43-45] gained recognition and confirmed by Rothrock and Waldron [39, 40] and Miller [48].

Total ignition delay comprises of physical ignition delay and chemical ignition delay. Physical ignition delay period dominates the initial stages leading to process like atomization of fuel spray, air entrainment, droplet formation, vaporization of fuel droplets and formation of air-fuel mixture. Chemical reactions takes over the physical ignition delay in the next half and hence known as Chemical ignition delay period. Although some chemical reactions takes place during physical ignition delay period but the rate of heat release during that period is insignificant as compared to the intensity and amount of heat release during chemical ignition delay period. Thus, there are two distinct physical and chemical ignition delay periods.

2.2 Physical Ignition Delay Period

Wenzel [49] in 1936, analyzed heating and vaporization process of fuel based on theory of similitude. According to which the time required for heating and complete vaporization of average drop of fuel is only a fraction compared to actual ignition delay.

That means ignition occurs in the fuel vapor and air mixture rather than on the surface of the drop. However, his results showed large variation when compared to experimental ignition delay values, which later he credited to wrong assumptions or occurrence of chemical delay as well.

In 1956, Yu, et al [50] conducted a study on physical ignition delay using single cylinder GM-71 engine. She injected nitrogen and fuel mixture in engine instead of fuel air mixture to measure change in pressure using hot-motored technique during alternate firing and misfiring cycles. It was observed that maximum drop in cylinder pressure was due to cetane number of fuel rather than its volatility.

In 1956, Hurn, et al [51] conducted experiments on fuel of different volatilities on a constant volume bomb at different charge temperatures to study the effect of charge temperature on fuel droplet heating and vaporization. A long delay was observed before measurement of actual chemical heat release, which they referred to initial lag before chemical reaction starts to heat and vaporize fuel drops. He observed and concluded that surrounding air has more effect on fuel droplet evaporation rather than fuel volatility and structure.

El-Wakil et al [52] in 1956, analyzed process after fuel injection i.e. fuel jet breakup and vaporization of atomized fuel in combustion bomb as well as diesel engine. They observed vaporization of fuel droplets under condition where adiabatic saturation occurs from edge to center of the spray. Under this condition, most of the fuels reach their autoignition temperature and fuel air ratio almost at the same time. They also found that pressure rise delay in engine is shorter than that of a constant volume combustor.

In 1968, experimental study conducted by Lyn and Valdmanis [53] to observe the effect of injection pressure, injection rate and nozzle size fetched them some unexpected results. They varied injection pressure from 200 to 350 atm and increased nozzle size from 0.3 mm to 0.6 mm, but there was no significant change in ignition delay period owing to a conclusion that auto ignition is a system property.

Henein [54] in 1971, studied vapor diffusion and mixture formation around evaporating fuel droplets. He defined ignition delay period as the time between start of heating up to the formation of a stoichiometric mixture at the ignition location around stagnant droplet. Using these assumptions physical ignition delay of 0.02 milliseconds was calculated for a 4μm Cetane droplet.

In 1974, Pedersen et al [55] developed a theoretical model for physical ignition delay based on single droplet calculations. They used the model to observe the effect of air pressure and temperature, fuel temperature, fuel mean droplet size and velocity on physical ignition delay. Like Lyn and Valdmanis, they also observed the effect of injection pressure and nozzle hole diameter on physical ignition delay and found similar results. Based on their study on evaporation of moving fuel droplet, they defined end of physical ignition delay as the time when stoichiometric mixture starts forming from moving droplet. They also found physical ignition delay value of 0.04 milliseconds at 1530 °R temperature.

Ryan [56], in 1985 observed a clear distinction in physical and chemical ignition delay period by injecting fuel with air and an inert gas (nitrogen) separately in a constant volume combustor. Absence of exothermic reactions when injected with nitrogen showed only physical ignition delay since there was no burning of fuel only droplet

evaporation and mixing. However when fuel was injected with air both physical and chemical ignition delay was observed. When cylinder pressure traces were superimposed on each other, the point of separation of pressure rise rate in air with pressure trace in nitrogen marked the end of physical ignition delay (Fig. 2.1). He observed that unlike ignition delay in diesel engine, in constant volume combustion chamber physical ignition delay accounts for a major part of total ignition delay.

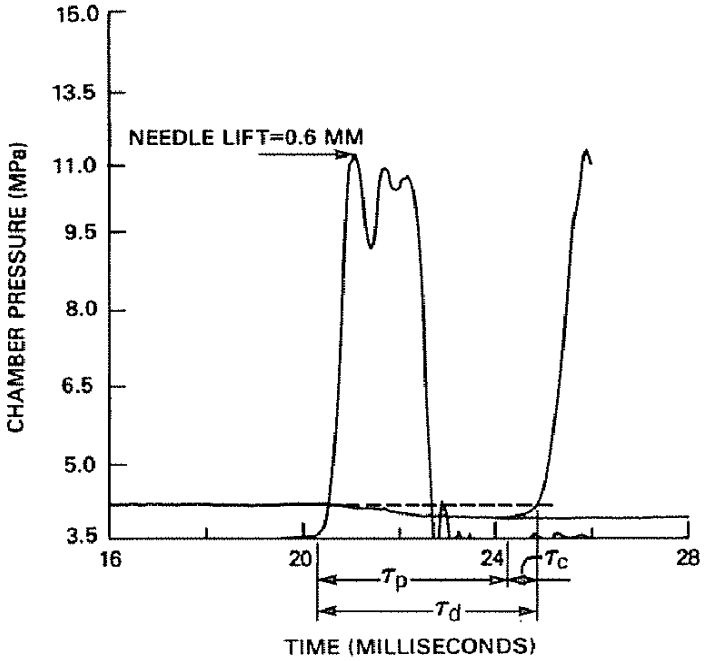

Figure 2.1: Pressure traces for a blend of Hexadecane and HMN in air and nitrogen [56]

From the ignition delay review, it is observed that, in engines physical ignition delay period is very small as compared to the chemical ignition delay period but for constant volume combustion chamber it accounts for major part of total ignition delay period.

2.3 Chemical Ignition Delay Period

From the start of simulation era, simulation has played major role in supporting study of Chemical ignition delay period. Dec [58] developed a conceptual model for studying ignition delay in diesel engines using laser sheet imaging and explained autoignition, combustion and emissions. Based on his study Flynn et al [57] developed chemical kinetics model for iso-octane and n-heptane to propose a structure for combustion in diesel engines. Both Dec and Flynn observed that the steps involved in autoignition process and the intermediate species formed during chemical reaction are similar for the fuels they used but the rate of reaction in formation of those intermediate species differ. Rate of reaction is affected by low temperature heat release and intermediate temperature heat release of these fuels [59].

Chen et al [60] as well as Westbrook [61] analyzed oxidation of hydrocarbons and categorized the process into Low temperature, Intermediate temperature and High temperature regimes.

2.3.1 Low Temperature Regime.

Low Temperature Regime is marked by reactions taking place below 850 K. Westbrook [61,62] et al explained hydrocarbon oxidation and low temperature branching in his works. According to him, alkyl radical (- R) is formed at low temperature when a hydrogen atom detaches from a hydrocarbon molecule.

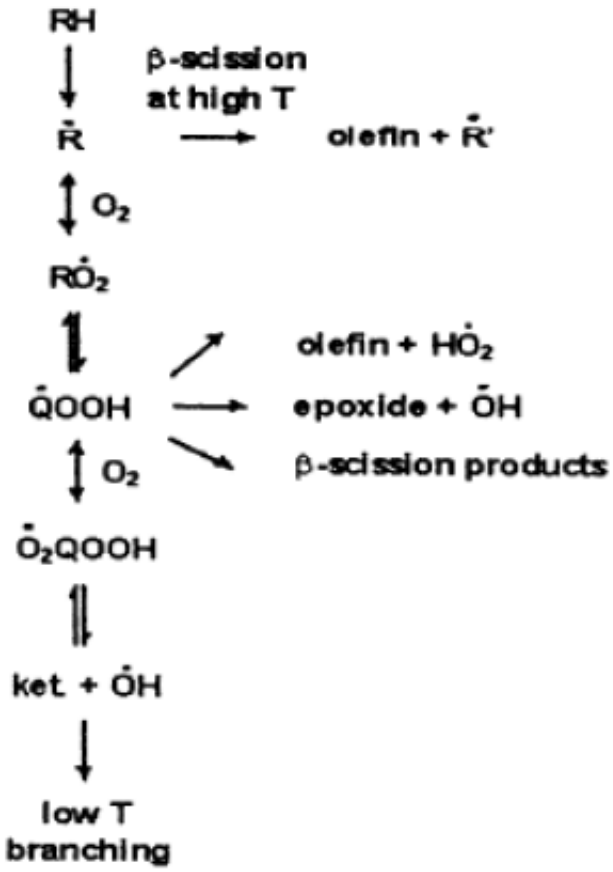

Figure 2.2: Schematic showing Hydrocarbon oxidation [61]

This alkyl radical combines with an oxygen molecule to form RO_2 molecule which later isomerizes to form QOOH radical where Q=C_nH2n.

$R + O_2 + M = RO_2 + M$ ……..(1)

$RO_2 = QOOH$ ……..... (2)

QOOH radical can either decompose or oxidize. Upon decomposition, it can either form Olefin and HO_2 molecule or cyclic ether and OH molecule.

Decomposition:

$QOOH = Q + HO_2$ ……..…… (3)

$QOOH = QO + OH$ ……..…… (4)

Oxidation:

$QOOH + O_2 = O_2QOOH$ …….……..... (5)

O_2QOOH further breaks into Ketohyroperaoxide and Hydroxyl molecule. Ketohydroperaoxide decomposes at around 800 K, which marks the end of Low Temperature Regime.

2.3.2 Intermediate Temperature Regime.

Intermediate Temperature Range is around 850 K to 1200 K. In this temperature range, OH formation takes place, which is used in high temperature range. OH formation is given by following reactions:

$H + O_2 + M = HO_2 + M$ …… (6)

$RH + HO_2 = R + H_2O_2$ ……..... (7)

$H_2O_2 + M = OH + OH + M$ ……. (8)

2.3.3 High Temperature Regime:

High Temperature Ranges above 1200 K. At temperature above 1200 K rate of OH formation increases and reaction (9) takes over OH formation rate at intermediate temperate range. Reaction for OH formation:

$H + O_2 = O + OH$ …….…….. (9)

Final reaction in combustion process is oxidation of CO and OH, which marks the end of High Temperature regime.

$CO + OH = CO_2 + H_2O$ ……. (10)

H atom for this reaction comes from decomposition of alkyl radical taking place at high temperature.

2.3.4 Negative Temperature Regime:

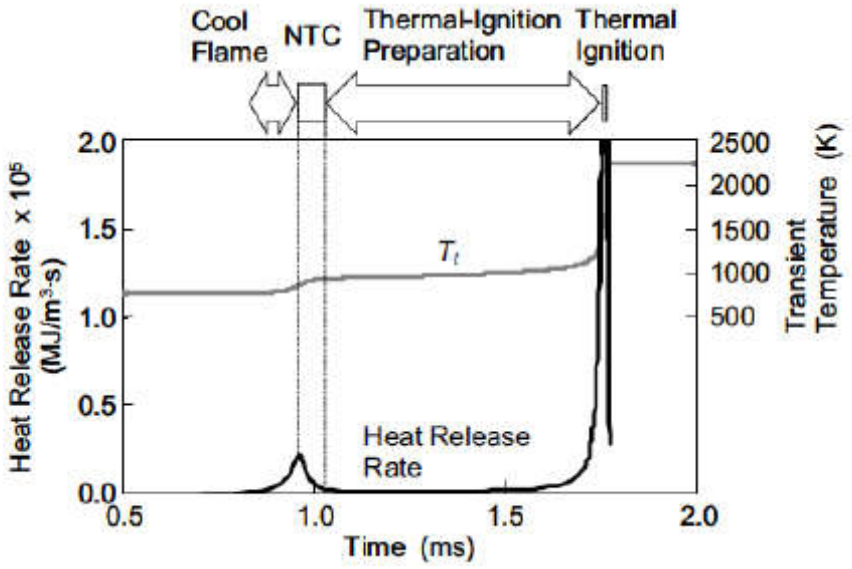

Figure 2.3. Different stages of auto ignition using Heat Release Rate [63]

In 2007, Kuwahara et al [63] proposed four stages of oxidation process (Fig. 2.3) for hydrocarbon fuels that showed cool flame before its combustion. It was based on the 0-D simulations using n-heptane and di-methyl ether. At high initial temperatures, O_2 addition reaction dominates cool flame. Transition from cool flame to NTC regime is marked by O_2 addition and OH subtraction, which results in byproducts like aldehydes and H_2O_2. At around 950 K, H_2O_2 loop reaction gets activated and controls transition of NTC regime to thermal ignition preparation stage. The H_2O_2 loop reaction recycles H_2O_2 and releases heat. The loop reaction consists of following reactions:

$H_2O_2 + M = 2\ OH + M$ ..... (11)

$OH + HCHO = HCO + H_2O$ ..... (12)

$HCO + O_2 = HO_2 + CO$ ..... (13)

$2\ HO_2 = H_2O_2 + O_2$ ..... (14)

The loop reaction releases around 473 kJ of energy, which aids in increasing temperature leading to high temperature combustion. When the temperature increases to 1500 K, there is transition of stage from thermal ignition preparation stage to thermal ignition stage.

2.4 Ignition Delay and Temperature effects on Ignition Delay

In 1931, Boerlage and Broeze [64] developed one of the early Ignition Delay co-relations based on experiments they conducted on single cylinder, four stroke, direct injection diesel engine at low rpm and pressure. They developed an equation for pressure rise as a function of compression pressure.

$$ID_P = \frac{K}{P} \tag{15}$$

Later, they compared combustion of Cetane ($C_{16}H_{32}$) and Tetra-isobutane ($C_{16}H_{32}$) [65] under similar conditions and observed that although both have similar chemical formula, cetane burns better than tetra-isobutane. Based on this result they concluded that, besides compression pressure even molecular structure plays important role in deciding ignition quality of fuel.

Wolfer [66] in 1938 developed relation for ignition delay based on the experiments he conducted on two different constant volume bomb of cylindrical and spherical shape. He considered pressure range of 8 - 27 bar for cylindrical bomb and 11 - 49 bar for spherical bomb with a common temperature range of 600 – 947 °F for fuels with CN more than 50. Equation is given by:

$$ID_P = \frac{0.44e^{\frac{4650}{T}}}{P^{1.19}} \tag{16}$$

Where P = Pressure in atmospheres and T = Temperature in °K

From his later experiments he concluded that injection pressure, nozzle diameter, turbulence, combustion chamber design, fuel air ratio and fuel temperature above 100°C have minimal effect on ignition delay values.

Schmidt [67] in 1939 derived a correlation for initial delay in chemical reaction between molecules of two gases but without considering intermediate reactions. Correlation is given by

$$ID_{Ch} = \frac{e^{+\frac{E}{RT}}\sqrt{T}}{P} a'B \tag{17}$$

Where, a' = factor which depends on air fuel ratio

B = factor responsible for reducing ignition delay from the increased rate of burning during the delay period due to temperature rise during the interval.

Further, to relate the equation to chemical ignition delay in engines, he applied exponential power to pressure to incorporate the effect of chain reactions during intermediate species formation. He noticed that exponential factors were more dominant than T, a' and B. Equation is given by

$$ID = \frac{ce^{\frac{b}{T}}}{P^n} \tag{18}$$

West and Taylor [68] in 1941 conducted experiments on single cylinder open chamber diesel engine and developed a correlation between ignition delay and T log P, as shown in Fig 2.4

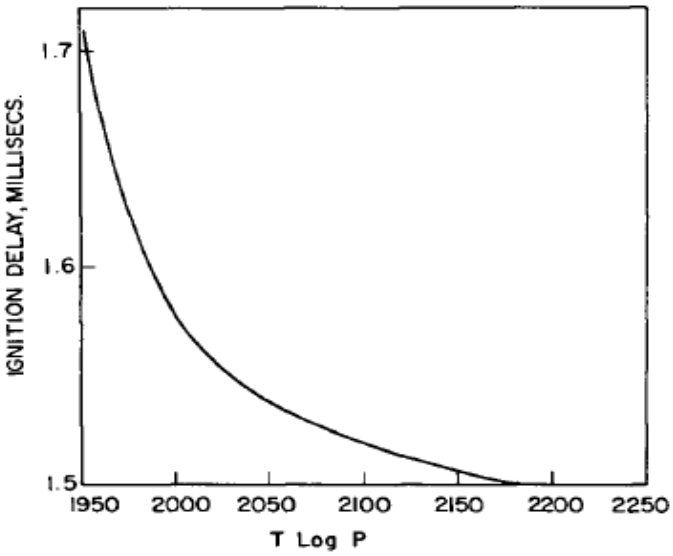

Figure 2.4: Correlation between Ignition delay and T log P [68]

Based on experimental data from Mueller [70], Wolfer [66] and Jost [71], Elliot [69] in 1949, derived a formula stating summation of physical and chemical ignition delay using relation between pressure rise delay and temperature.

For methylnaphthalene the formula is:

$$ID = 0.977e^{\frac{107\,0}{T}} + 2.18 \times 10^{-1\,4}e^{\frac{14510}{T}} \tag{19}$$

For cetane the formula is:

$$ID = 0.710e^{\frac{1\,07\,0}{T}} + 3.47 \times 10^{-1\,4}e^{\frac{1\,7\,6\,2\,0}{T}} \tag{20}$$

In 1956, Hurn et al [72] injected fuels with different volatilities in constant volume bomb to study the factors affecting fuel evaporation and chemical heat release during autoignition process. They observed that chemical heat release occurred after short delay following fuel evaporation and this time delay was affected by physical properties of fuels. Fuel volatility and chemical structure of fuel had less impact on heat transfer rate to fuel droplet during physical ignition delay but chemical ignition delay was affected by chemical composition of fuel.

Yu et al [73] obtained similar results for effect of fuel volatility by conducting experiments on single cylinder engine to study change in pressure during ignition delay period. They observed that maximum pressure drop is dependent on CN of fuel.

El-Wakil et al [74] in 1956, analyzed the path between SOI and end of pressure rise delay. They also studied effect of spray breakup process and concluded that spray breakup will not affect physical ignition delay significantly. From one of the important study they concluded that constant volume bomb has longer pressure rise delay compared to engine.

In 1967, Henein and Bolt [75] conducted experiments on single cylinder diesel engine to study the effect of cylinder pressure, fuel air ratio, injection pressure, cooling water temperature and turbulence on illumination delay and pressure rise delay. Both the delays are affected mostly by air pressure, fuel air ratio and cooling water temperature. It is observed that illumination delay has longer duration and is more sensitive to injection pressure than pressure rise delay. They derived an empirical relation for ignition delay

$$ID_P = \frac{C}{P^n} \tag{21}$$

Where C = 64740 and P^n = 1.774

In their further study in 1969, they studied the effect of air charge temperature on pressure rise of different cetane number fuels like gasoline, CITE and diesel. Low cetane number fuel showed large drop in ignition delay values due to increase in air charge temperature than high cetane number fuel. But at extremely high temperatures, ignition delay of all the fuels are less sensitive to rise in intake temperature and show close resemblance in their values as shown in fig 2.5

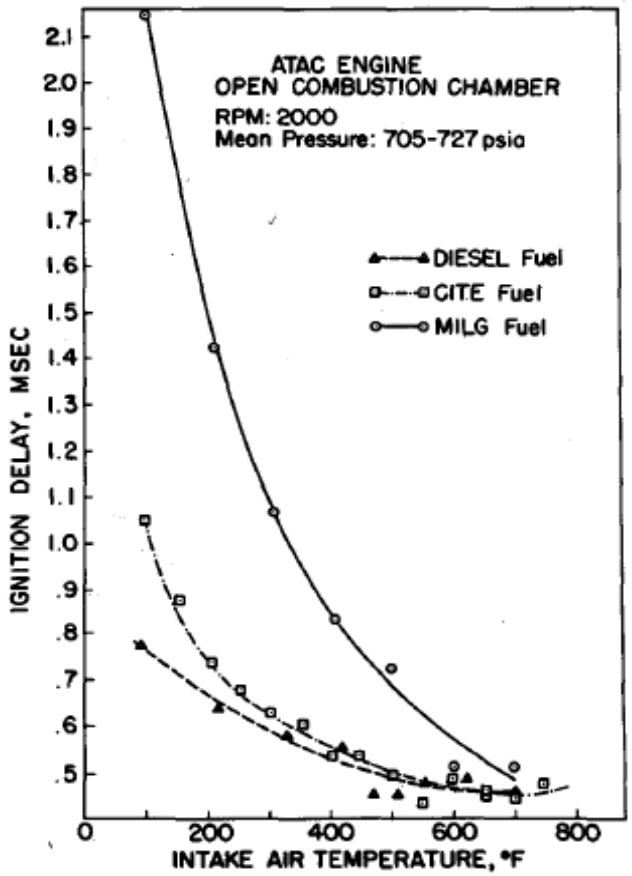

Figure 2.5: Effect of intake air temperature on ignition delay of different CN fuels [76]

In 2000, Siebers et al. [77] performed experiments on a constant volume combustion chamber with optical diagnostics tools to study the effect of intake air temperature and charge density on premixed combustion of diesel fuel. As intake air temperature is varied from 800 to 1000K, average equivalence ratio increased and autoignition started at an equivalence ratio of about 4 at 1100K. Whereas with increase in density from 7.27 to 45 kg/m^3, air entrainment rate in fuel increased. This leads to high air fuel mixture temperature and early autoignition with reduced ignition delay.

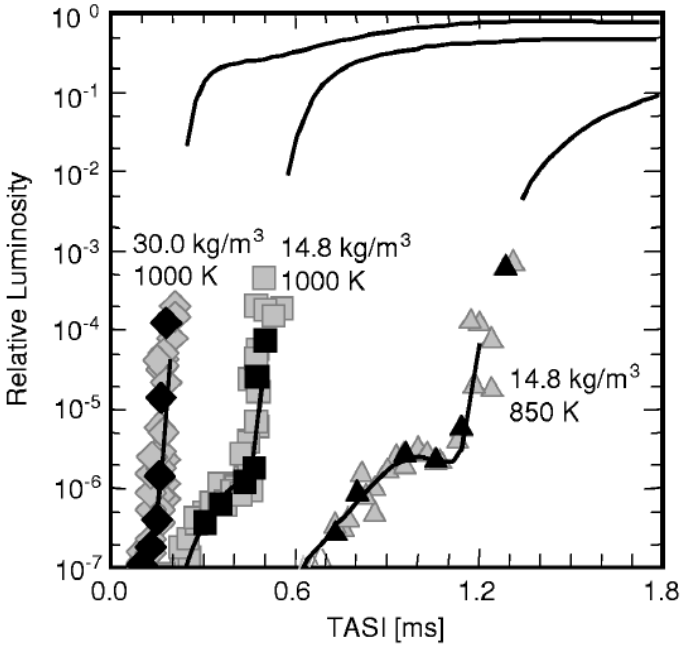

Figure 2.6: Relative luminosity under different temperatures and densities [77]

Fig. 2.6 above shows Relative luminosity of diesel versus time After Start of Injection (TASI) at three different charge densities and temperatures. Density of 14.8 Kg/m3 and 1000K temperature is considered baseline condition. It is observed that as ambient temperature decreases from 1000K to 850K at constant baseline condition density, two stage combustion occurs and becomes more significant. However when ambient density is increased from 14.8 to 30 kg/m3, two stage combustion vanishes. So the auto ignition location changes with increase in gas density. They concluded, NTC is a process where overall reaction rate of combustion decreases even with increasing temperature [78]. Heat released during first stage and increasing temperature controls the transition between stages. As ambient temperature and density decreases, reaction rate decreases and ignition delay increases and as ambient temperature and density increases ignition delay decreases significantly.

In 2005, Pickett et. al. [79] conducted similar study. They analyzed the chemiluminescence of diesel fuel jet in optically equipped constant volume combustion chamber.

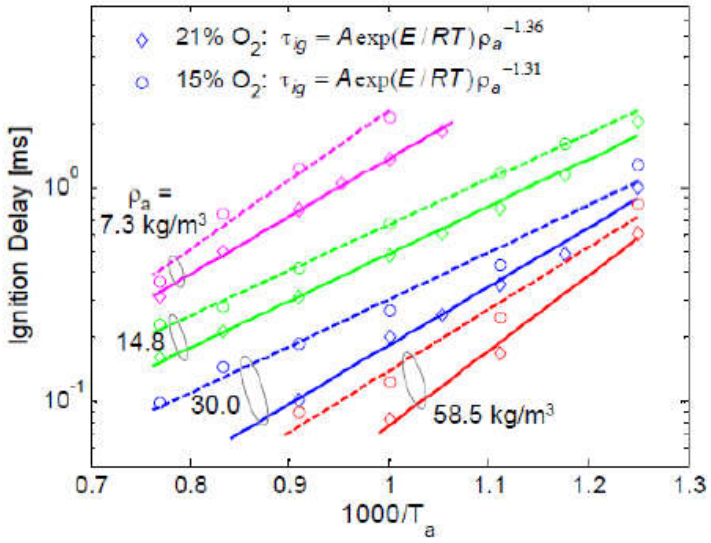

Figure 2.7: Ignition Delay versus 1/temperature at ambient condition [79]

Conditions for results in Fig. 2.7 are 180μm orifice, 11380 bar pressure drop, fuel at 436K and oxygen concentration 15% and 21%. From the experimental results in Fig.2.7, they concluded that ignition delay decreases when ambient temperature increases at constant charge density, decreases when charge density increases at a given temperature and decreases when percentage of oxygen in charge density increases.

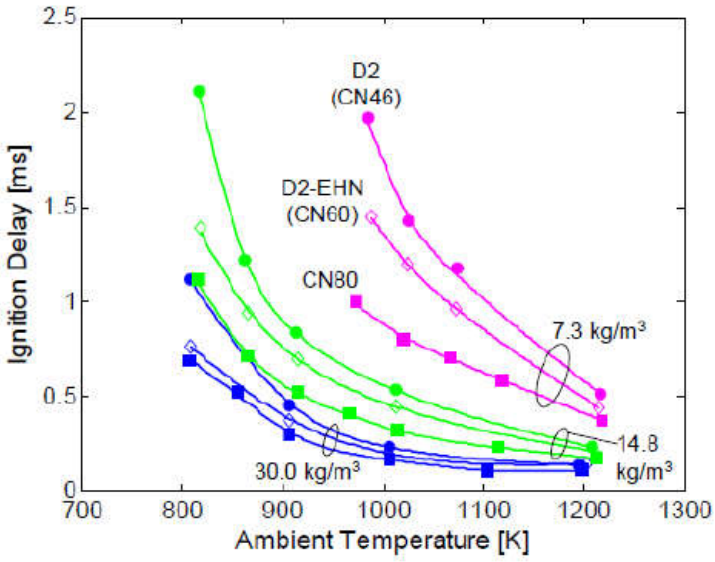

Figure 2.8: Ignition Delay versus 1/temperature at different conditions [79]

Conditions for results in Fig. 2.8 are 180μm orifice, 11380 bar pressure drop, fuel at 373K and oxygen concentration 21%. Fig. 2.8 shows at high temperature and charge density ignition delay is significantly less sensitive to cetane number.

Pickett et. al. in 2008 conducted experiments using constant volume combustion chamber to study liquid lengths of Diesel and JP8. Both the fuels were injected at fuel temperature of 436K using 0.246mm nozzle for Diesel and 0.18mm nozzle for JP-8. The test results showed, when charge density and ambient temperature is increased, liquid lengths of both the fuels decreases as shown in Fig. 2.9. They also observed that low boiling point of JP-8 accounts for its early evaporation and shorter liquid length.

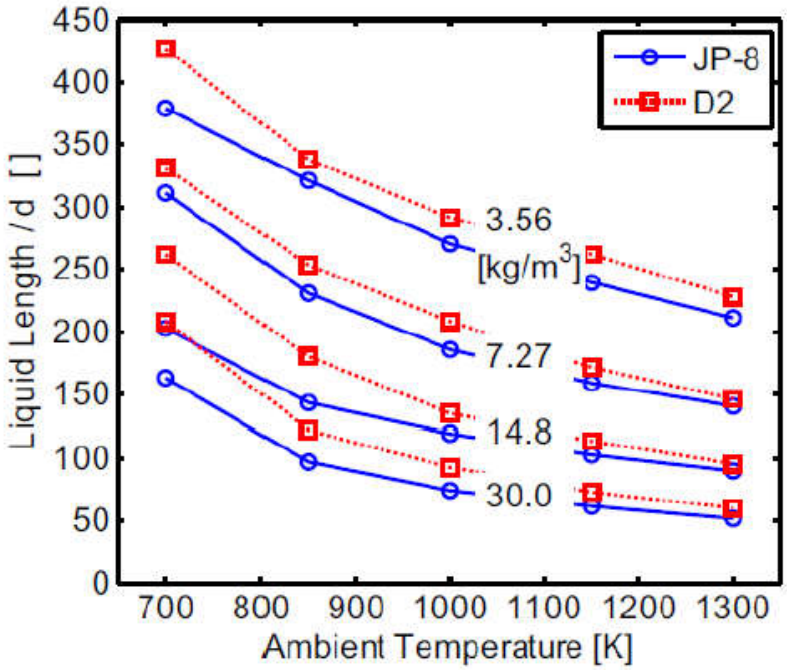

Figure 2.9: Liquid lengths of Diesel and JP-8 at different temperatures and charge densities. [79]

In the same year Takada et. al. [80] conducted CFD simulation to simulate effects of intake air temperature, pressure and EGR on various characteristics of rate of heat release trace. They observed specific characteristics of rate of heat release mentioned in Fig. 2.10 and the base line conditions they considered for the experiments mentioned in Table 2.1

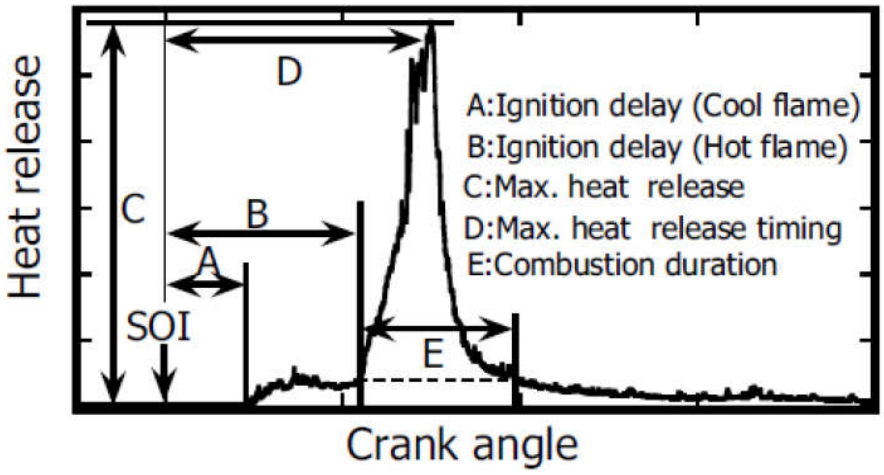

Figure 2.10: Characteristics parameters of Rate of Heat Release [80]

Engine speed rpm	2000
Intake pressure kPa	100
Fuel injection timing deg. ATDC	0 (TDC)
Fuel quantity mm^3/st	20
EGR ratio %	19.1
Intake O_2 concentration vol%	18.5
Intake gas temperature K	344.7

Table 2.1: Baseline test conditions [80]

Based on the simulation results shown in Fig. 2.11, they observed that cool flame is not significantly affected by intake air temperature, hot flame ignition timing is advanced and combustion duration reduces with increase in the intake air temperature.

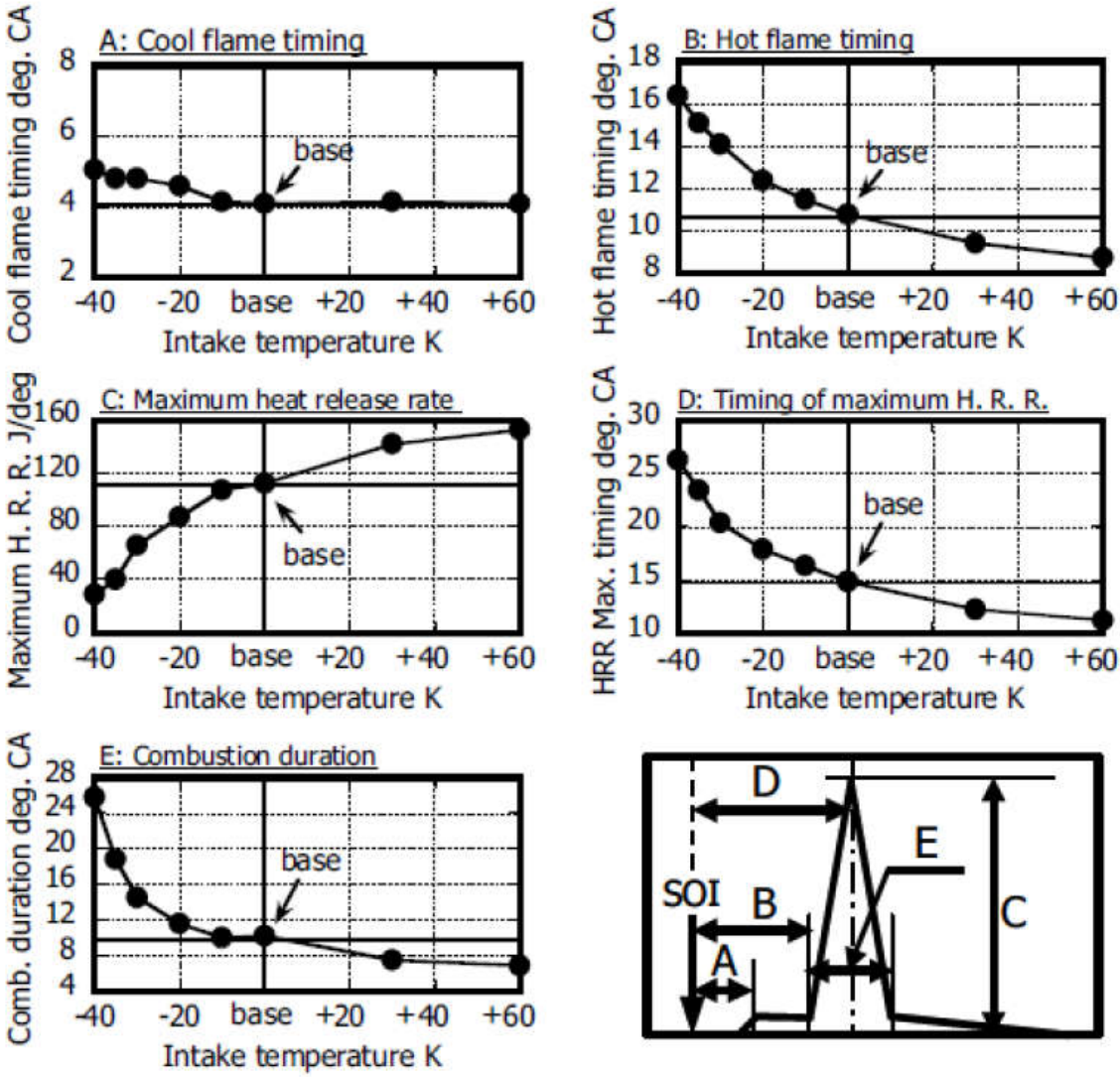

Figure 2.11: Effect of intake temperature on Rate of Heat Release parameters [80]

In 2013, Jaykumar [81] showed the effects of different loads and intake air temperatures on behavior of NTC regime for low cetane JP-8 fuel on a single cylinder diesel engine. He considered two test conditions, low intake temperature, low load (50°C, 3bar IMEP) and high intake temperature, high load (110°C, 5bar IMEP). Fig. 2.12 shows experimental results at different loads and intake air temperatures.

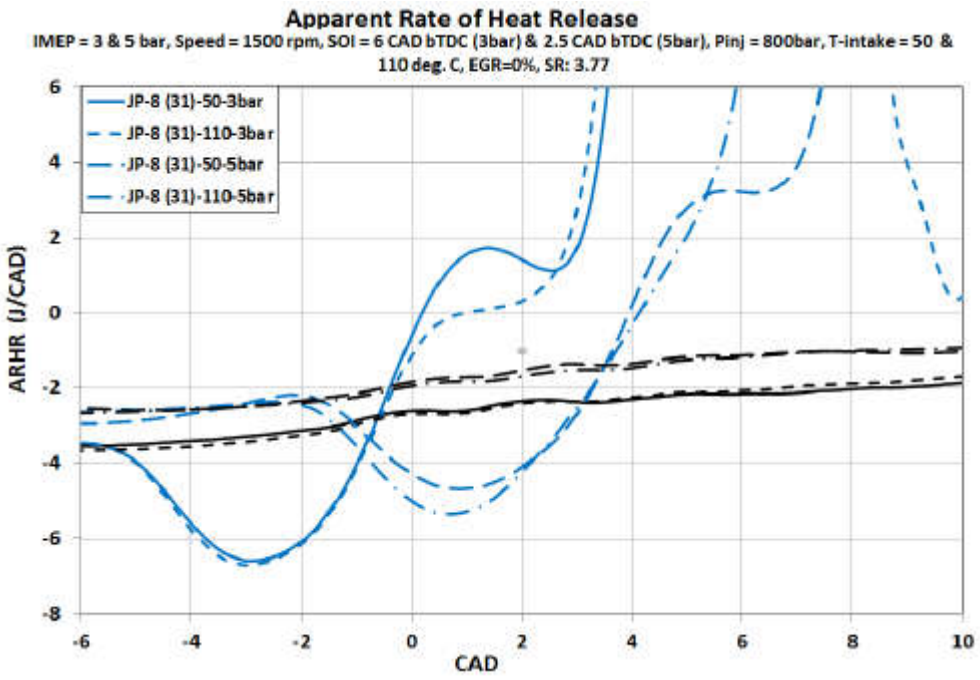

Figure 2.12: Effect of intake temperature and load on NTC regime [81]

He observed, at low load and low intake temperature NTC regime is very significant. With increase in temperature NTC regime at low load, NTC regime disappears but cool flame remains. At high load NTC regime is significant but not as significant as low load. When intake temperature is increased at high load, NTC regime and cool flame both disappears.

The literature review shows that studies have been conducted on effect of intake air temperature on autoignition. But this thesis the combined effect of Start Of Injection (SOI) and varying intake air temperature on NTC regime of low cetane SASOL IPK is investigated. Batch to batch variation also affects the cetane number of fuel which in turn affects the autoignition and combustion of fuel. This report focuses on low cetane number SASOL IPK with a DCN of 31.17

CHAPTER 3

EXPERIMENTAL SETUP

3.1 Engine Test Cell Setup

Test cell engine setup consists of a single cylinder Diesel engine coupled with a DC dynamometer, which is used, for speed and load control of engine. The test engine gets air supply at intake plenum from a compressed air tank, which acts as a super charger providing compressed air for effective combustion and providing control over intake air pressure. An air heater on inlet line controlled intake air temperature. Independent cooling system of engine includes cooling tower and radiator which supplies distilled water to water jacket around engine maintaining a set engine wall temperature. Also, a water supply from city water is used for cooling fuel pump and oil pump separately. Lubrication system consist of oil pump supplying oil for cooling piston and for lubricating cams. Engine is equipped with Common Rail fuel injection system which maintains constant fuel pressure throughout. Two fuel pumps are used to attain required fuel pressure. Fuel injection strategy in the engine is controlled by an open ECU which gives a precise control on fuel injection quantity. Data Acquisition System collects pressure signals from pressure transducers as input and gives in cylinder pressure RHR and Temperature as output. From the exhaust side two outlets are taken for emission measurements. One outlet to Horiba test bench for exhaust gas analysis and other outlet to SMPS for Particulate Matter analysis. All the above mentioned systems are explained in details in following pages.

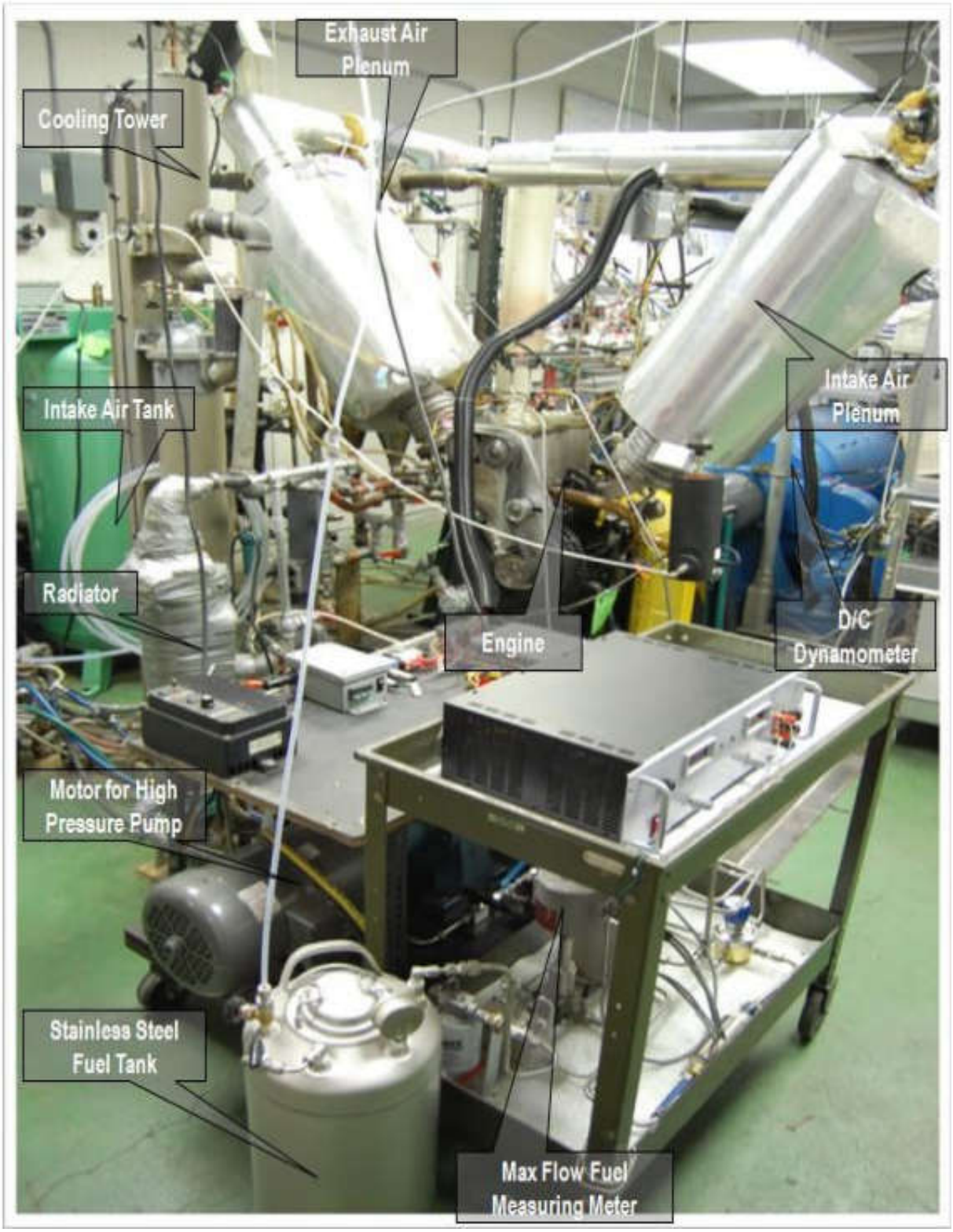

Figure 3.1: Picture of PNGV test cell [82]

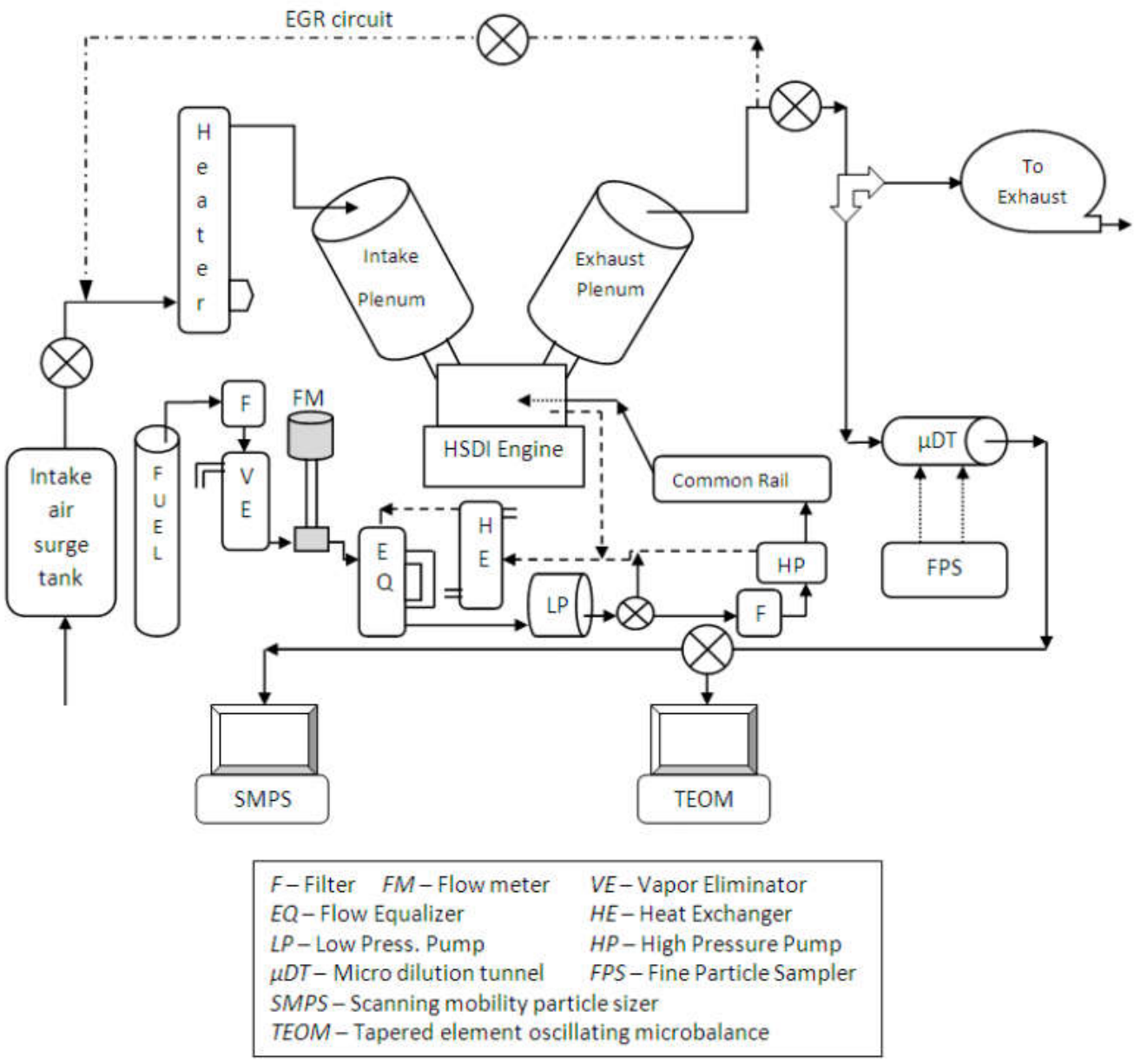

Figure 3.2: Schematic diagram of the complete experimental setup [82]

3.2 Engine Specification

Engine installed in PNGV lab is 0.42 liter, custom made four stroke, Single Cylinder, High Speed Diesel Test Engine with Double Over Head Cams. The inlet manifold incorporates two swirl ports which enables user to vary the swirl ratio inside

combustion chamber. Engines Mexican hat type piston and aluminum cylinder head is made my Ricardo. Test engine is fitted with open ECU to control the fuel injection event precisely, likewise all engines systems can be controlled individually to control the intake conditions. The engine specification are mentioned in table 3.1

Engine Type	Four Stroke Diesel
Number of Cylinders	1
Displaced Volume	421.932 cc
Stroke	85 mm
Bore	79.5 mm
Connecting Rod	179 mm
Crank Radius	42.5 mm
Bowl Diameter	36.25 mm
Geometric Compression ratio	20:1
Number of Valves	4
Inlet Valve Open	353°
Intake valve Close	-140°
Exhaust Valve Open	155°
Exhaust Valve Close	-352°
Nozzle type and size	320 Minisac, Ø 0.131 mm, 6 holes
Spray angle	145°

Table 3.1: Table showing engine specifications [82]

3.3 Intake Air System

Air is supplied to the engine under controlled pressure and temperature. It is compressed by a two stage compressor and stored in air tank at the basement. Air flow from the high pressure air tank is diverted to two paths, one to the surge tank which supplies air to engine air intake and other to the exhaust measurement device Fine Particle Sizer for dilution of exhaust. Air in the surge tank reduces fluctuation in airflow and fetches compressed air to the intake plenum giving a turbocharger effect. Intake plenum is insulated to reduce heat losses to atmosphere. Air pressure can be controlled by a valve at the outlet of the surge tank. Intake air line also has manually controlled heater to heat the air entering the intake manifold.

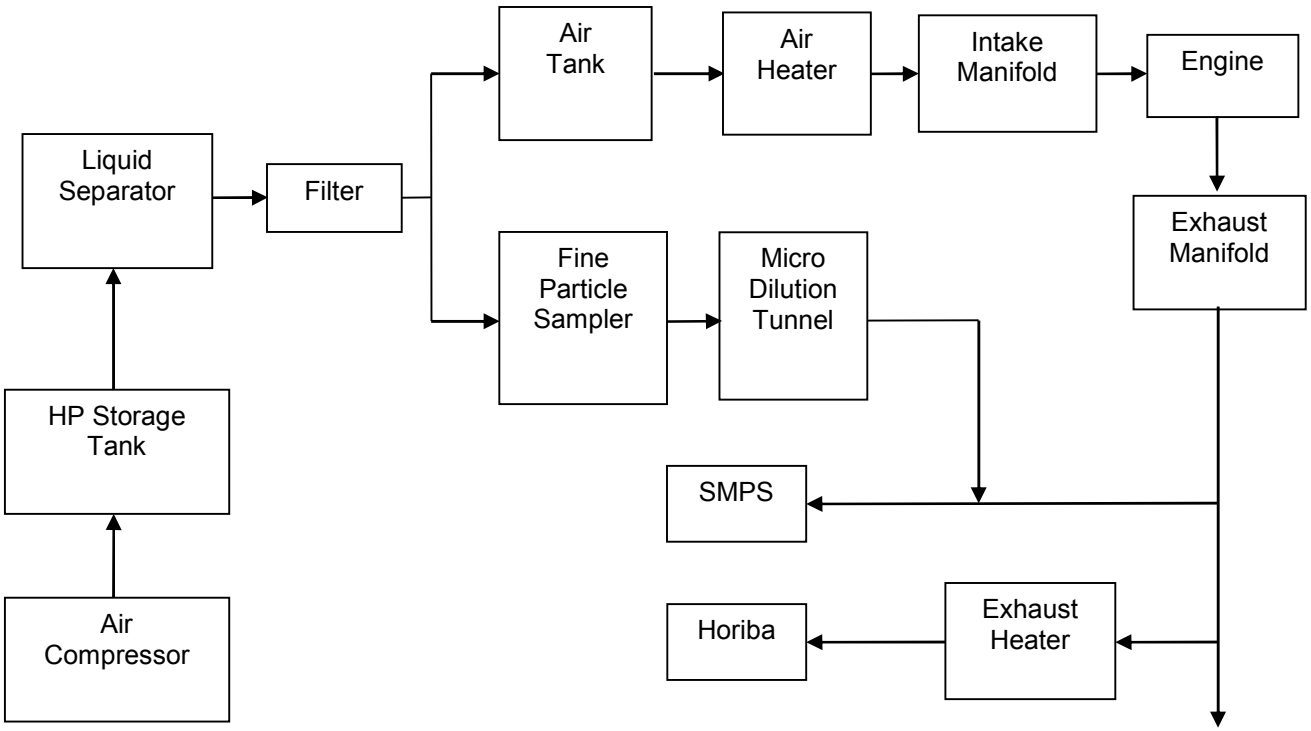

Figure 3.3: Schematic diagram showing Intake Air flow in the system [83]

3.4 Engine Cooling System

City water was used as a coolant for cooling engine. Two city water supplies were used, one for cooling engine and fuel line and other supply for cooling engine oil from oil sump through a shell and tube heat exchanger. The engine cooling line splits into two lines one going to cylinder head jacket and other to the wall jacket or engine block. The engine block temperature was kept constant by controlling the coolant flow and steam flow such that water outlet temperature from engine remains 180 °F. Temperature range was maintained with ± 1°F. For maintaining constant water outlet temperature steam line was used to heat the water entering engine block. For measuring temperatures at the inlet and outlet of water 'K' Type thermocouples were used.

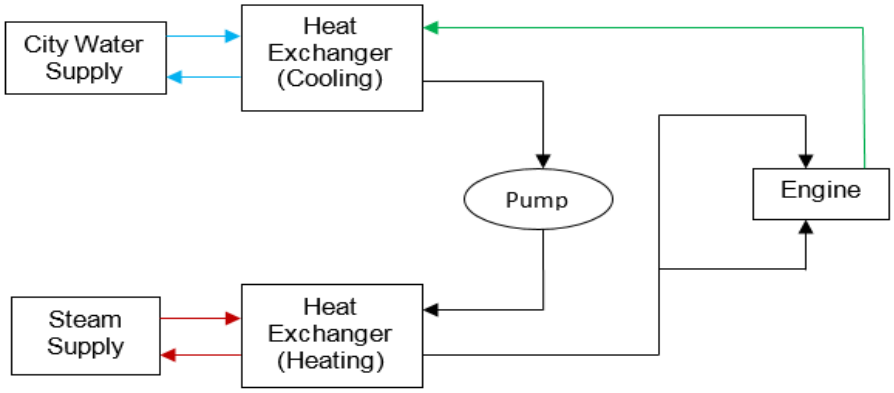

Figure 3.4: Schematic diagram of the Engine cooling system [83]

3.5 Oil flow in the System

There is exclusive engine oil system for engine which runs independently providing proper lubrication to the engine. Oil system consist of two heat exchangers, an oil pump and oil filter. Two heat exchangers connected in series maintains the

temperature of engine oil in the system at 120°F. At this temperature viscosity of oil decreases providing required lubrication. Oil before entering the engine passes through an oil filter and then oil line splits in to two. One lines goes to cylinder head providing lubrication to cams and connected components and the other line enters from the bottom of the engine block forming piston jet lubricating cylinder walls and piston. Oil from both the lines drains down to the oil sump at the bottom of the engine. From there it is again recirculated through return line, heat exchangers and oil pump.

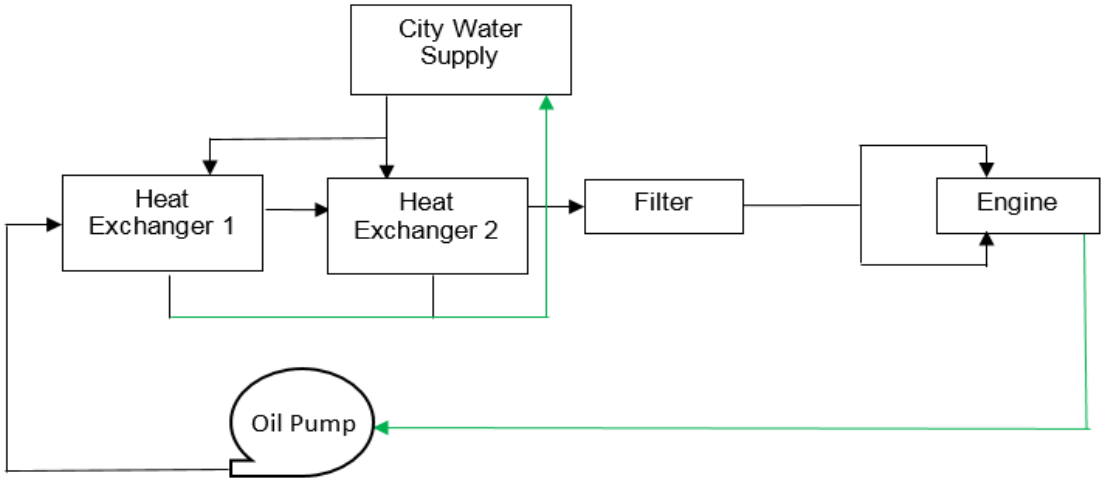

Figure 3.5: Schematic diagram showing Oil flow in the system

3.6 Fuel System

The fuel system used here is Common Rail Direct Injection system capable of generating max pressure of 1350 bars. Main componenets of fuel system are pressurized fuel tank, fuel filter, fuel flow meter, low pressure fuel pump, high pressure fuel pump, common rail system and return line with heat exchanger. Fuel is kept in pressurized stainless steel tank to prevent evaporation, it also aids in smooth functioning of Low pressure fuel pump. Between fuel tank and low pressure pump there

is fuel filter to filter out solid impurities, vapour eliminator which eliminates any bubbles in the line, flow meter to measure the flow using pressure difference and flow equalizer which provides constant flow or constant level of fuel before it enters low pressure pump. Low pressure pump maintains 2bar pressure at its outlet and directs fuel through pressure regulator to a high pressure fuel pump. Pressure regulator maintains a constant pressure of 2bar at its outlet irrespective of any flow variation at the low pressure pump. In case of low pressure pump malfunction excess pressure can be releaved through bypass line preventing any damage to high pressure fuel pump. High pressure fuel pump maintains the pressure required in the common rail. Open ECU controls the pressure in common rail through high pressure fuel pump. It also controls the fuel injection timing and duration, so accordingly injector can have pre and/or main injection. But this experiment was conducted only using main injection. Injector returns the extra fuel through a return line. From there fuel passes through a heat exchanger to cool the compressed fuel and then it again enters in Flow Equalizer to maintain constant flow.

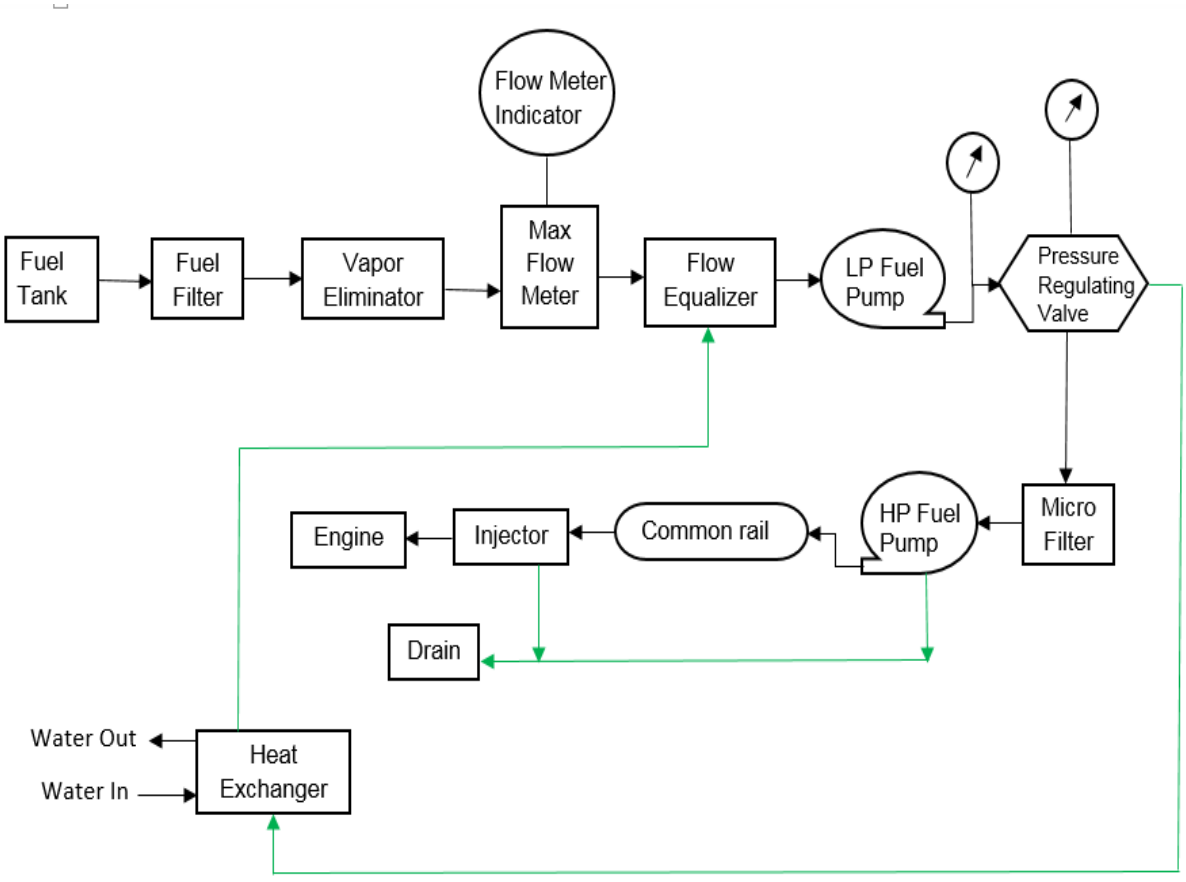

Figure 3.6: Schematic diagram of Fuel delivery system

3.7 Data Acquisition System

Hi-Tech Data Acquisition with Win 600 software is used to collect data from the engine. Inputs used by data acquisistion system are:

a) Encoder signal from encoder mounted on engine crank.

b) In cyclinder pressure signal from water cooled Kistler pressure transducer mounted on top of cylinderhead.

c) Pressure transducer mounted on fuel common rail.

d) Intake pressure and temperature readings.

Outputs from Data Acquisition System are (Output is average of 70 cycles) :

a) In cyclinder pressure trace.
b) Average Rate of heat release.
c) Mass average temperature.

In cylinder temperature is calculated using Ideal Gas Law taking into consideration the assumption that temperature is uniform throughout the combustion chamber and temperature calculations are valid from Intake Valve Closing to Exhaust Valve Opening. Temperature calculation is shown below:

$$\frac{P\ (intake) * V\ (intake)}{n\ (intake) *\ \bar{R} * T\ (intake)} = \frac{P\ (\theta) * V\ (\theta)}{n\ (\theta) *\ \bar{R} * T\ (\theta)}$$

Rearranging the terms we get,

$$T\ (\theta) = \frac{P\ (\theta) * V\ (\theta) *\ T\ (intake)}{P\ (intake) * V\ (intake)}$$

Where molar ratio ie. $n\ (intake)/n\ (\theta)$ is considered to be unity and *P, V, T, n* are pressure, volume, temperature and number of moles respectively; $\bar{R}$ is Universal Gas Constant; intake denotes conditions during intake; θ is the crank angle degree at any given point of time.

Rate of Heat Release is calculated using the correlation mentioned in Win600 software user manual:

$$\frac{dQ}{d\theta} = \frac{n}{n-1} *\ P\frac{dV}{d\theta} + \frac{1}{n-1} * V\frac{dP}{d\theta}$$

Where Q is the Rate of Heat Release; θ is crank angle degree; n is polytropic constant; *P,V* are pressure and volume respectively.

3.8 Target Fuel

Target fuel used for experiments is a Coal to Liquid derived, Iso Paraffinic Kerosene [101,102] fuel produced by SASOL company. It is obtained by Fischer-Tropsh process [95-100] which converts mixture of hydrogen and carbon monoxide obtained from coal, methane or biomass into liquid fuels by means of gasification. SASOL IPK is a low cetane number fuel (CN: 25.4). Its properties are mentioned in Appendix A.

CHAPTER 4

IGNITION DELAY DEFINITIONS

Ignition delay (ID) is defined as the time (or crank angle) interval between the start of injection (SOI) and start of combustion (SOC) [3]. There is general agreement between past researchers that ID period starts with SOI, which is measured from needle lift of the injector [3]. Some researchers have also used start of injector energizing [24] and pressure drop in fuel pressure trace [84] for defining SOI. For this report, drop in fuel pressure trace is used for defining SOI.

The end of ID period is determined by the SOC. Determination of location of the SOC varies with the researcher and the kind of fuel used for experiments. Some researchers define SOC as the point where rate of heat release (RHR) trace crosses zero and becomes negative to positive [17, 31, 85-88]. These definitions were used for high cetane number fuels and failed to take into consideration the two-stage combustion that occurs due to negative temperature coefficient regime (NTC) and cool flame in the autoignition of low cetane number fuels.

In recent times, researchers have come up with SOC definitions which takes into account NTC and cool flame for low cetane number fuels. These definitions [89, 90-93] are based on the cumulative rate of heat release (CuRHR) instead of RHR. Definitions based on CuRHR defines SOC with three approaches mentioned below.

- The point where CuRHR trace crosses zero.
- The point where 5% mass burn fraction occurs and lies at 5% (CA5) of CuRHR

- The point where 10% mass burn fraction occurs and lies at 10% (CA5) of CuRHR

These definitions takes into account NTC regime, cool flame and pressure recovery point observed in constant volume combustion chambers. The CuRHR rise point matches with pressure rise point and hence in this report SOC using the CuRHR definition is used. Fig 4.1, shows the different ID definitions based on SOC using CuRHR trace.

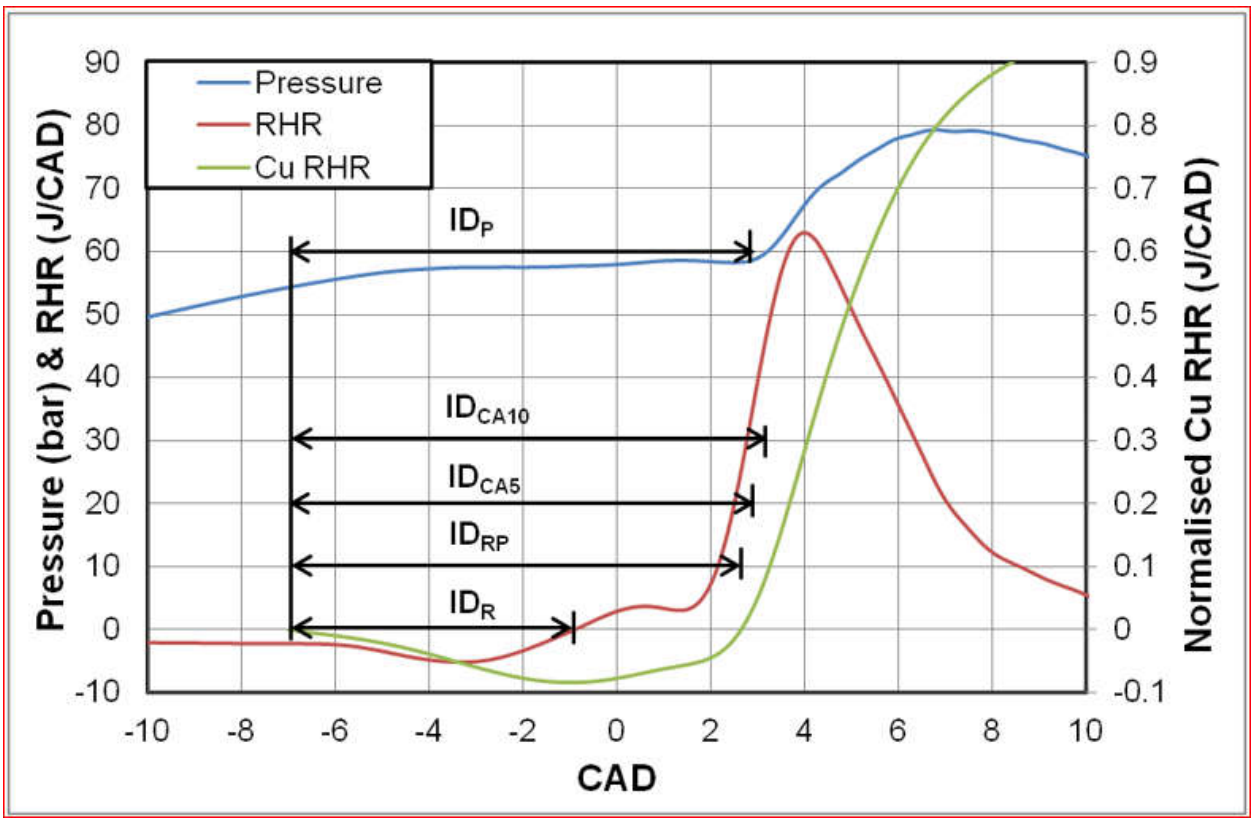

Figure 4.1: ID Definitions comparison using CuRHR trace [83]

1. ID_P = delay between SOI and start of pressure rise.
2. ID_R = delay between SOI and RHR trace crossing zero.
3. ID_{CA5} = delay between SOI and 5% of CuRHR curve.
4. ID_{CA10} = delay between SOI and 10% of CuRHR curve.

5. ID_{RP} = delay between SOI and CuRHR trace crossing zero.

For this report, the ID_{RP} definition is used for calculating ID at all the data points and for calculating Activation Energy (E_a) of fuel. E_a of fuel is calculated using the Arrhenius Equation, which gives correlation between ID and E_a.

$$ID = Ae^{\frac{E_a}{RT_m}} \quad \text{..... (4.1)}$$

ID = Ignition delay

A = Constant which depends on the fuel and combustion system characteristics

R_u = Universal gas constant

E_a = Apparent activation energy

T_m = Mean temperature

CHAPTER 5

RESULTS

SASOL IPK is analyzed for two cases

- Case 1: Varying inlet air temperature at three different injection timings
- Case 2: Varying Injection timing at a fixed intake air temperature.

For both cases, the equivalence ratio was maintained constant by changing the intake air pressure in accordance with the change in intake air temperature. To study the sensitivity of auto ignition and combustion quality of a fuel with respect to change in temperature, either Intake Air Temperature or SOI can be varied.

Table 5.1 shows, the minimum data points considered for analysis. The minimum number of points are selected because the same points will be considered for SASOL IPK surrogate validation in the future scope of the research. Due to cost limitations, minimum points will be considered for surrogate validation of SASOL IPK on a single cylinder diesel engine.

SOI (CAD)	T_{intake} (°C)
- 2	70
	90
	110
- 4	30
	50
	70
	90
	110
- 6	30
	50
	70

Table 5.1: Data points at different SOI and Inlet Temperatures

At all the data points considered for the study, the following parameters were kept constant.

- Fuel injection pressure (P_{inj}) of 800 bar.
- IMEP of 3 bar.
- Swirl ratio of 3.77
- Engine speed of 1500 rpm.
- Charge density.

For near TDC SOI of -2 CAD, the lowest intake air temperature considered is 70°C, because at lower temperatures, ignition delay of SASOL IPK will be fairly long and combustion will occur late in the expansion stroke, where the drop in temperature is severe and it would be difficult to correlate between the ID and charge temperature. On the other hand, for more advanced SOI at -6 CAD, the intake temperature is limited because of the high cylinder gas pressures reached after combustion. At higher intake temperatures, the intake pressure is increased to keep a constant charge density.

5.1. Effect of varying Intake Air Temperature (Constant SOI)

For this case, effect of intake air temperature on in-cylinder pressure, temperature and rate of heat release traces are investigated at each of the three SOI conditions.

5.1. a

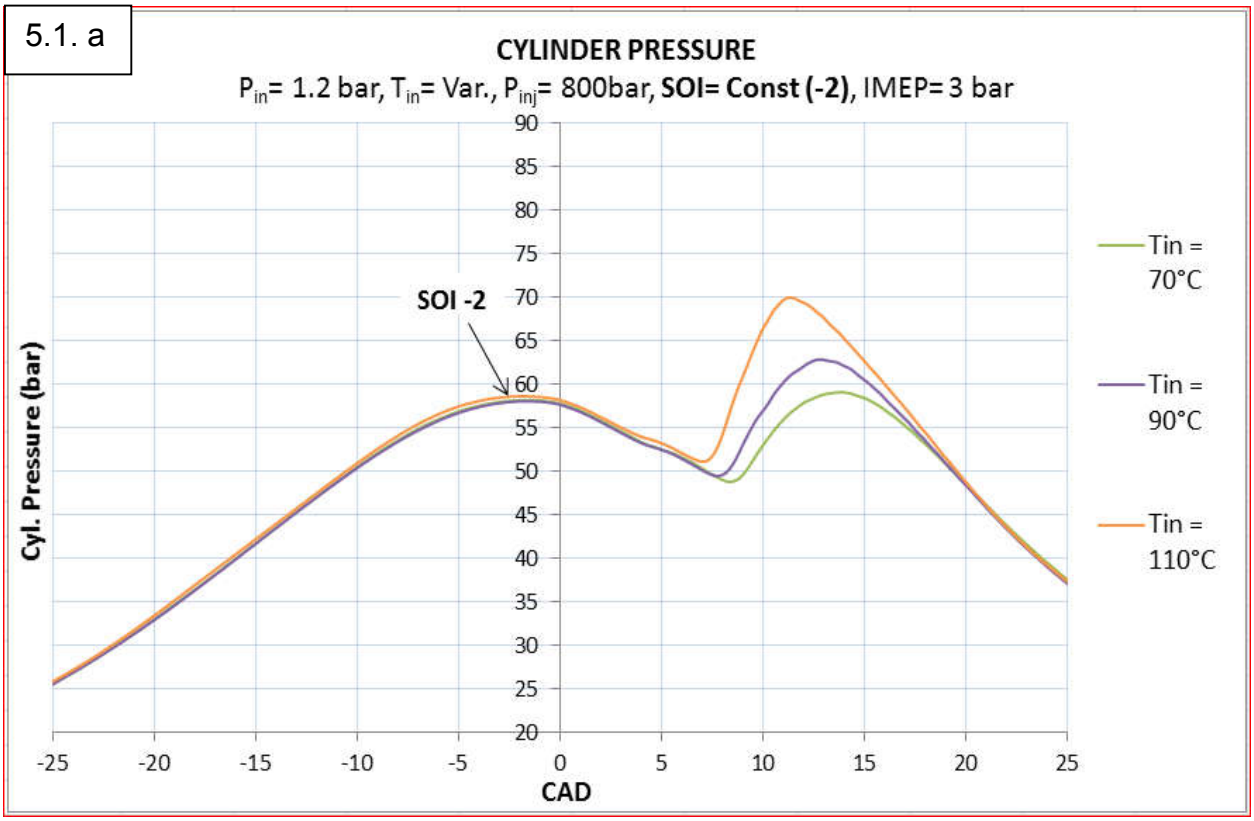

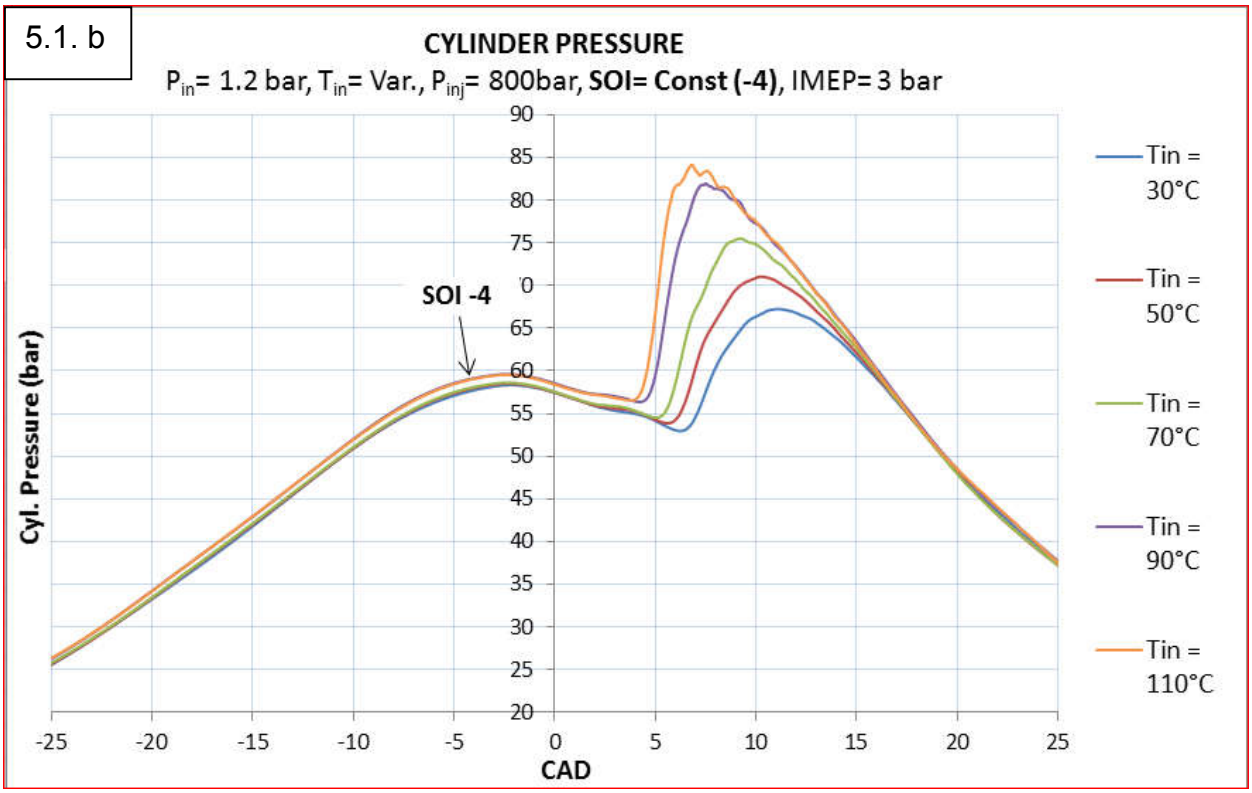

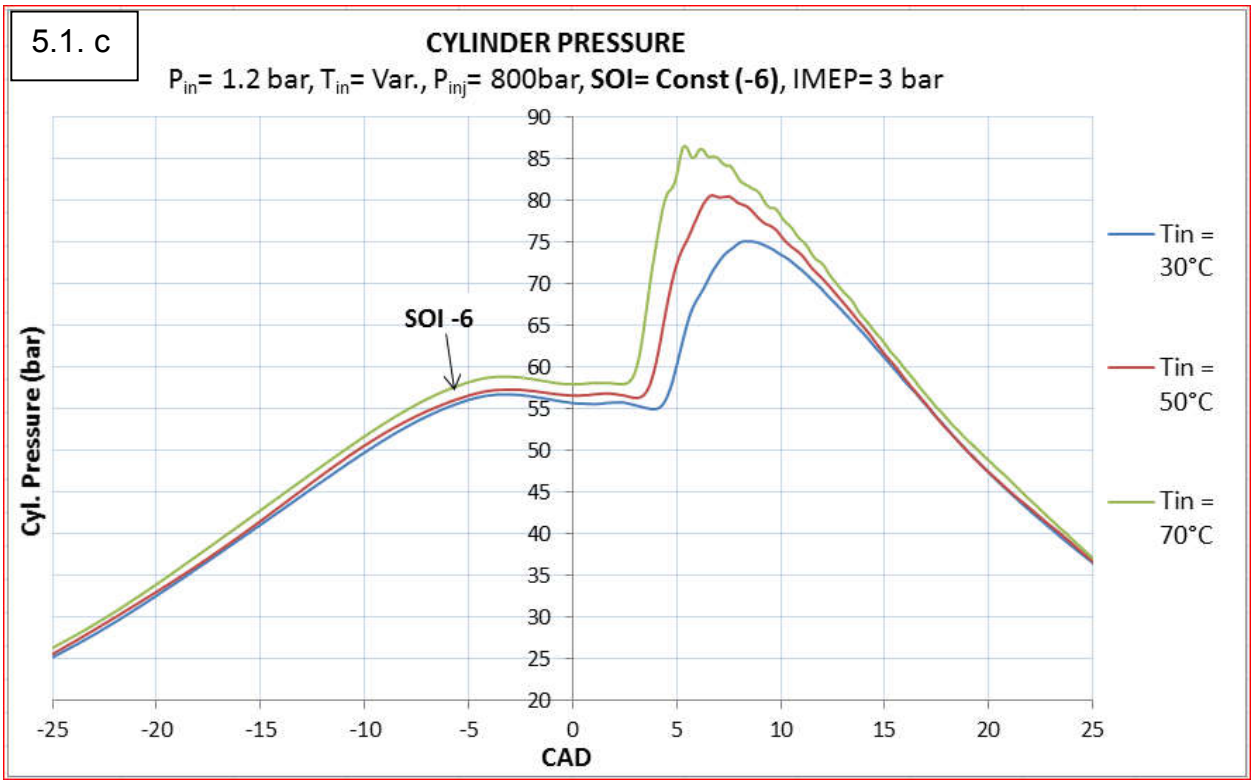

Figure 5.1: Comparison of pressure traces at SOI of -2, -4 and -6 CAD

5.1.1. Effect of varying Intake Air Temperature on In-cylinder Pressure.

Figure 5.1. shows comparison of pressure traces for SOI -2, -4 and -6 CAD. At each SOI, intake air temperature was varied and intake air pressure (P_{int}) was adjusted to keep charge density constant. The reason for selecting the different intake temperature points at different SOI is discussed earlier in this report. Fig 5.1.a. shows, at SOI -2 and T_{int} = 70°C, pressure generated is not high enough to contribute towards useful work. The cylinder pressure generated at this T_{int} is almost equal to motoring pressure because combustion started late in the expansion stroke which dropped the gas temperature. However, as the intake air temperature was increased to 110°C, start of combustion advanced towards TDC leading to pressure rise of up to 70 bar.

In Fig 5.1.b, for SOI of -4 CAD, the fuel is injected earlier than in figure 5.1.a and the peak pressure at T_{int} of 110°C reached 84 bar, which is around 14 bar higher than that reached at -2 CAD SOI . Many trends are observed in Fig. 5.1.a, 5.1.b, 5.1.c.

1. The peak cylinder gas pressure as well as the rate of pressure rise increase as SOI is advanced from -2 to -6. This is observed at all the inlet air temperatures, and is due to the shorter ID which causes combustion to start closer to TDC where cylinder gas temperatures are still high, before they drop in the expansion stroke.
2. The peak cylinder gas pressure as well as the rate of pressure rise increase at higher inlet air temperatures. This is observed at all the injection timings and is due to the shorter ID at the higher intake temperatures, which causes

combustion to start closer to TDC where cylinder gas temperatures are still high, before they drop in the expansion stroke. To TDC

3. The location of the peak cylinder gas pressure relative to TDC follows the same trend as the start of combustion. As stated in items (1) and (2) the start of combustion is advanced at earlier injection timings and higher inlet air temperature.

4. For more advanced SOI like -4 and -6, more cycle-to-cycle variation was observed in the peak pressure, at the higher intake temperatures.

5.1.2. Effect of varying Intake Air Temperature on In-cylinder Temperature.

As the in cylinder temperature is derived from in cylinder pressure trace using ideal gas law, temperature traces show similar trends as the pressure traces, with respect to peak temperature, location of start of temperature rise and peak temperature relative to TDC and rate of temperature rise. Temperature traces for different T_{int} at different SOI are given in Fig. 5.2.

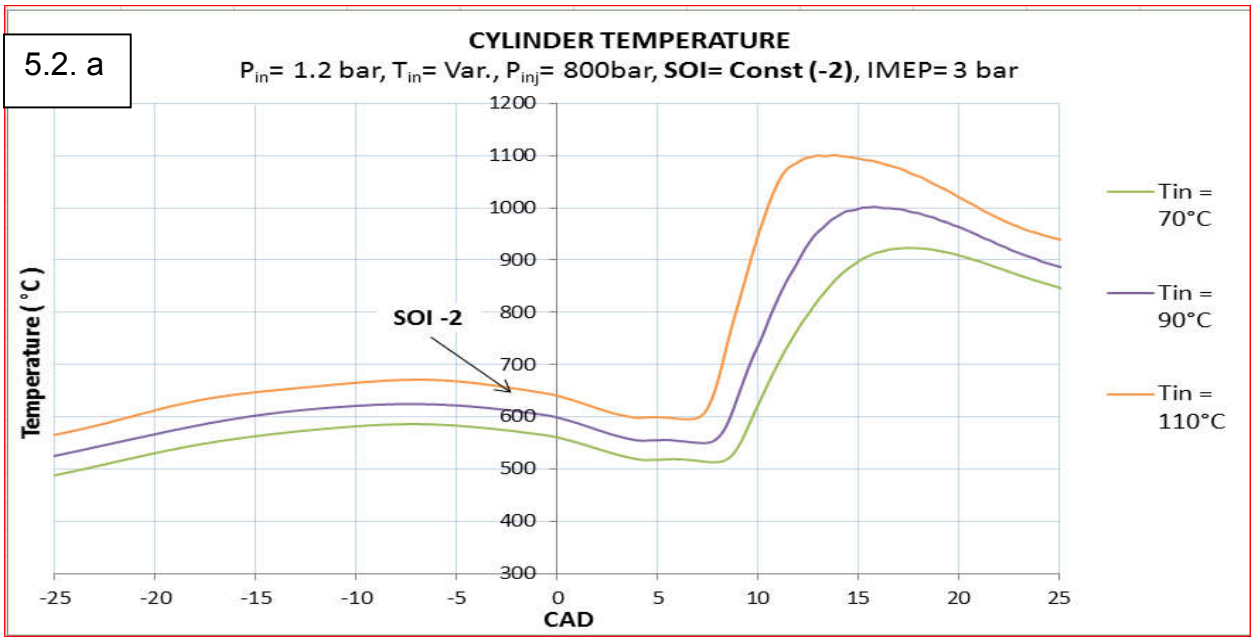

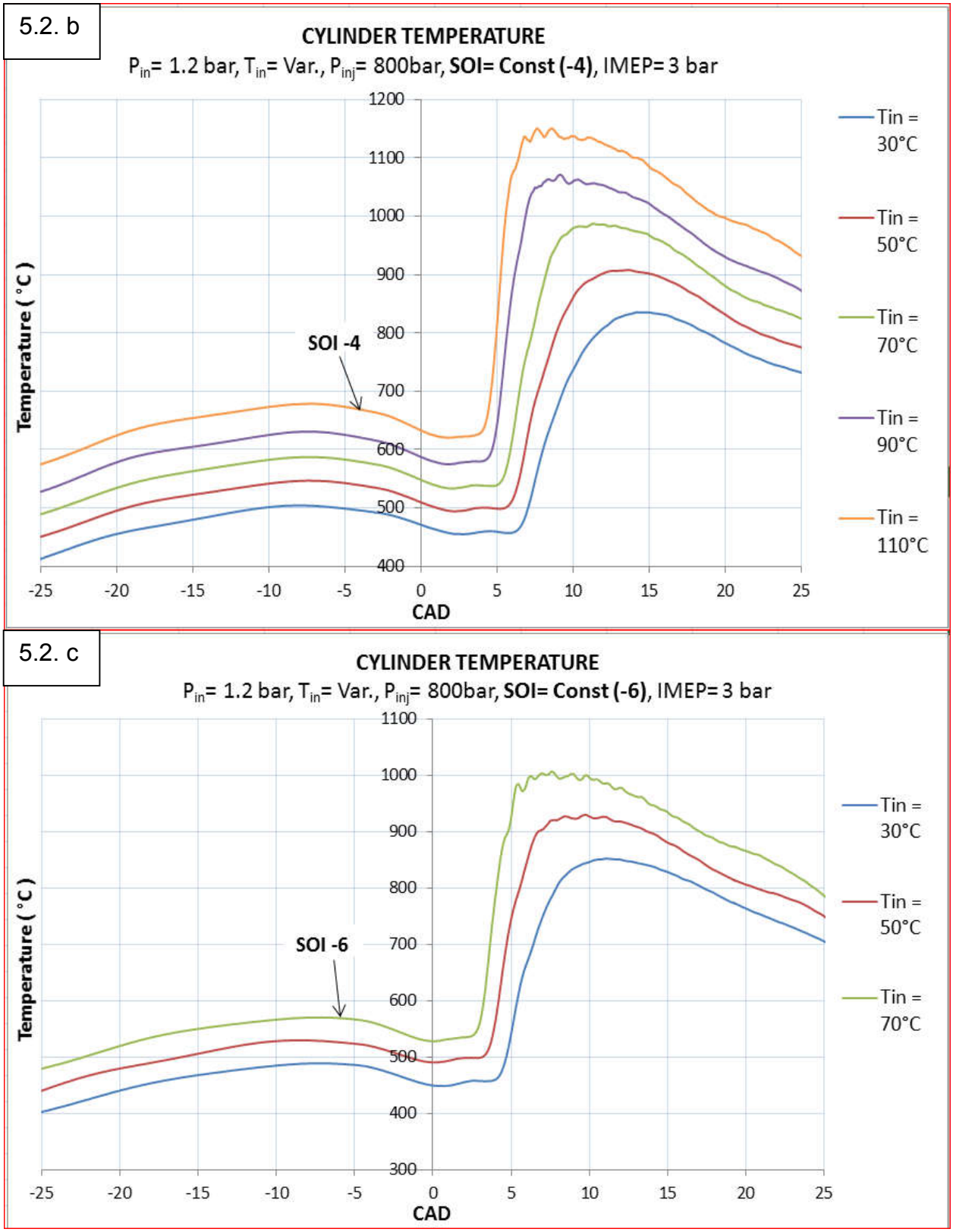

Figure 5.2: Comparison of temperature traces at SOI of -2, -4 and -6 CAD

5.1.3. Effect of varying Intake Air Temperature on Rate of Heat Release

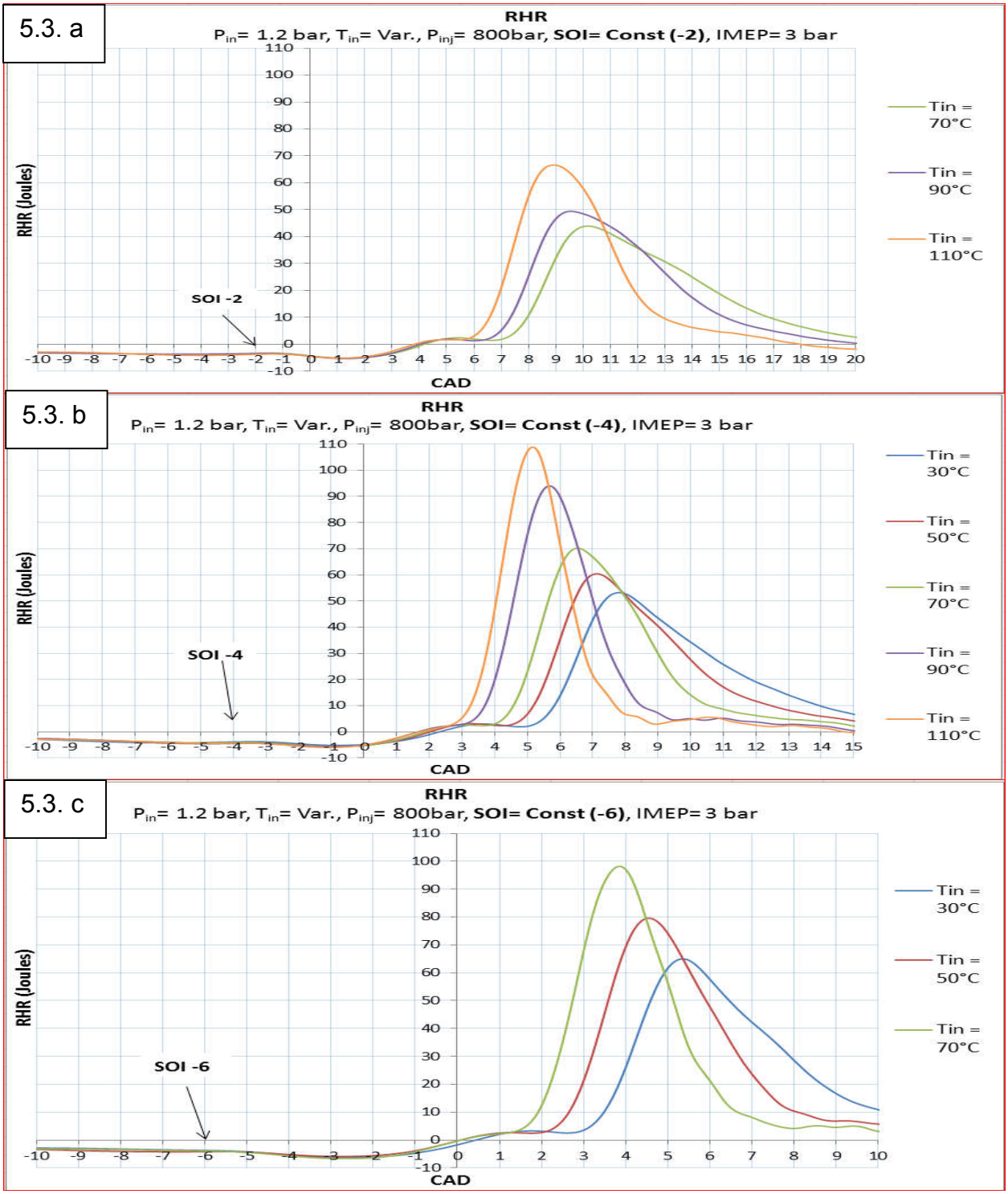

Figure 5.3: Effect of temperature on RHR traces at SOI of -2, -4 and -6 CAD

	SOI (CAD)

	-2			-4					-6		
Tin (°C)	70	90	110	30	50	70	90	110	30	50	70
ID (ms)	1.19	1.12	1.03	1.17	1.11	1.04	0.93	0.89	1.14	1.04	0.97
ID (CAD)	10.7	10.1	9.25	10.5	10	9.35	8.35	8	10.3	9.4	8.75
% Reduction in ID	0	5.88	13.4	0	5.13	11.1	20.5	23.9	0	8.77	14.9

Table 5.2.: Reduction in ID as an effect of T_{int} at SOI of -2, -4 and -6 CAD

Table 5.2. above shows the reduction in ignition delay values in milliseconds, CAD and percentage as the intake air temperature is increased for every SOI. Calculation of ID and definitions considered for calculating ID are explained later in Section 5.1.5.

Fig 5.3.a. and Table 5.2., show that for SOI -2, when T_{int} was increased from 70°C to 110°C, ignition delay of SASOL IPK decreased from 1.19 ms to 1.03 ms. Therefore peak of the RHR shifts towards TDC with a higher rate of increase and decay.

Fig 5.3.b shows, for SOI -4 when T_{int} was increased from 30°C to 110°C, ignition delay value of SASOL IPK decreased from 1.17 ms to 0.89 ms. From table 5.2. it can be seen that ignition delay value gradually decreases with increase in intake air temperature. This is because as intake temperature increases, evaporation rate of the fuel spray and mixing with air increases.

Fig 5.3. c, shows similar trends to figure 5.3.a and 5.3.b.

5.1.4. Effect of varying Intake Air Temperature on NTC Regime and Cool Flame.

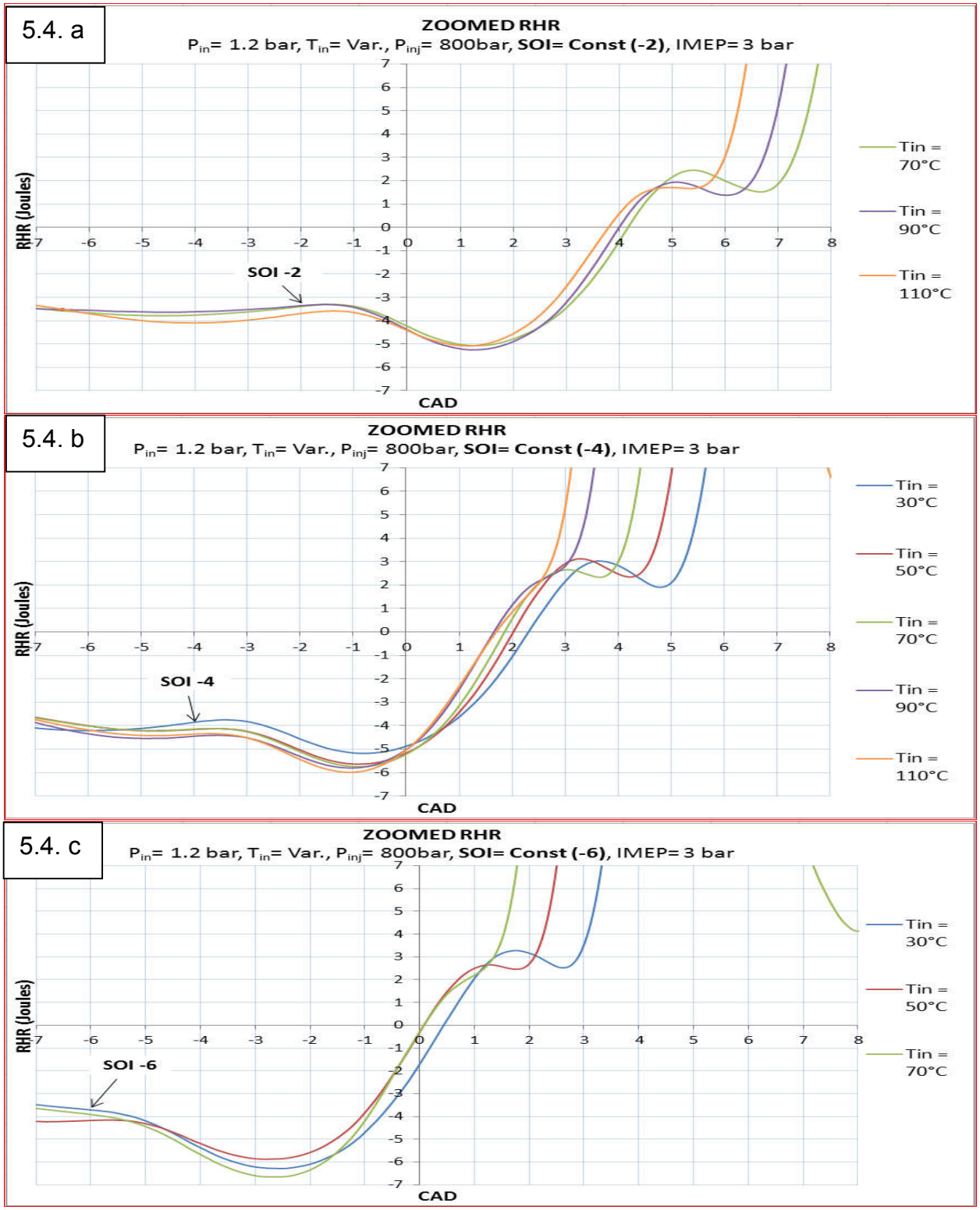

Figure 5.4: Effect of temperature on RHR (zoomed) traces at SOI -2, -4 and -6 CAD

Fig 5.4. shows the effect of temperature on RHR at different SOI. Zoomed RHR is considered to observe the effect of intake air temperature on NTC regime and Cool flame at different SOI. Both NTC regime and Cool flame are found to occur in intermediate temperature zones between 800 K and 1200 K. NTC occurs due to aldehyde formation at the start of combustion, which prolongs the autoignition of remaining fuel. RHR increases when exothermic reaction starts after fuel evaporation. However, this increase in RHR is followed by drop in slope due to aldehyde formation until sufficient amount of heat is released to oxidize aldehydes. After oxidation of aldehydes, heat release rate again increases marking start of combustion (SOC).

In Fig. 5.4.a, for SOI -2, as T_{int} is increased from 70°C to 110°C, there is no significant change in NTC regime or cool flame until 90°C. Above 90°C, as T_{int} approaches 110°C, NTC diminishes leaving behind only cool flame. Cool Flame starts from the point where the heat release rate starts rising due to exothermic reaction i.e. from around 1.5 CAD and continues until the point where the combustion reaction overcomes NTC regime and rise in RHR starts. As T_{int} increases the initial rise of RHR decreases, showing increased rate of oxidation of aldehydes with increase in intake air temperature.

In Fig. 5.4.b. for SOI -4, as T_{int} is increased from 30°C to 110°C, there is significant change in NTC regime and cool flame above 70°C. At T_{int} of 90°C, the NTC regime decreases drastically due to high charge temperature and only small quantity of cool flame remains. But as intake air temperature reaches 110°C, both NTC regime and Cool flame diminishes, depicting a RHR curve of high cetane number fuel.

In Fig. 5.4.c, for SOI -6, as T_{int} is increased from 30°C to 70°C, RHR shows a similar trend as seen for RHR at SOI -2 from 70°C to 110°C. At 30°C and 50°C, no significant change is noticed but as T_{int} reaches 110°C, NTC regime disappears and cool flame is highly reduced because ID decreases due to increase in intake air temperature.

5.1.5. Observations based on the Zoomed RHR Graph

Fig. 5.4.a and Fig. 5.4.b, show that at a high temperature of 110°C, the point where exothermic reaction takes over endothermic reactions i.e. the lowest point in the drop of RHR after the SOI, shifts by 2 CAD towards TDC. In addition the value of lowest point on the drop of RHR decreases by around 1 Joule, indicating higher rate of endothermic reaction with advancing SOI. The rate of rise of the RHR curve also becomes steeper when SOI is advanced.

A comparison of RHR traces for 70°C in Fig. 5.4.b and Fig. 5.4.c shows that, the point where exothermic reaction starts, is shifted more towards compression stroke by around 1.5 CAD. Consequently, as the SOI is advanced, the fuel evaporation rate increases as seen from steeper drop due to endothermic reaction. However, it should be noted that even by advancing SOI, the time between SOI and the end of endothermic reactions remains constant for all the SOI.

5.1.6. Ignition Delay Determination at varying intake air temperatures

The ID_{RP} definition mentioned in Chapter 4 is used to determine ID values for the data points given in table 5.1. SOI is considered as the start of ID period and SOC as the end of ID period. SOC is determined by the point where CuRHR crosses zero i.e. the CuRHR recovery point which matches with the start of pressure rise point. When the

CuRHR recovery point is plotted on RHR trace, it takes into consideration the NTC regime and cool flame. IDCA5 and IDCA10 defnitions are not used in this report because when these points are plotted on RHR trace it corresponds to the stage where most of the combustion has already occurred and RHR trace is near its peak value. Fig.5.5. shows ID determination for SOI -2, -4 and -6 at varying intake air temperatures.

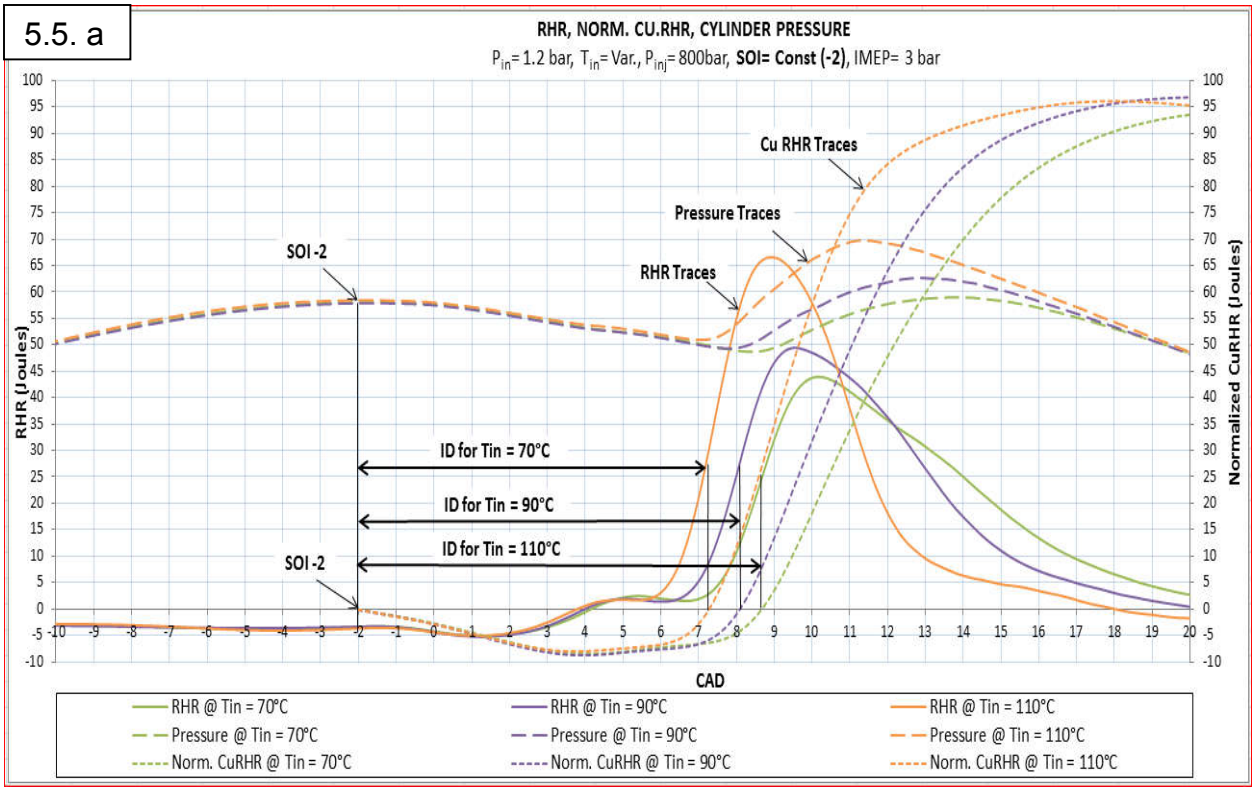

Figure 5.5.a : ID determination for SOI -2 with varying intake air temperature

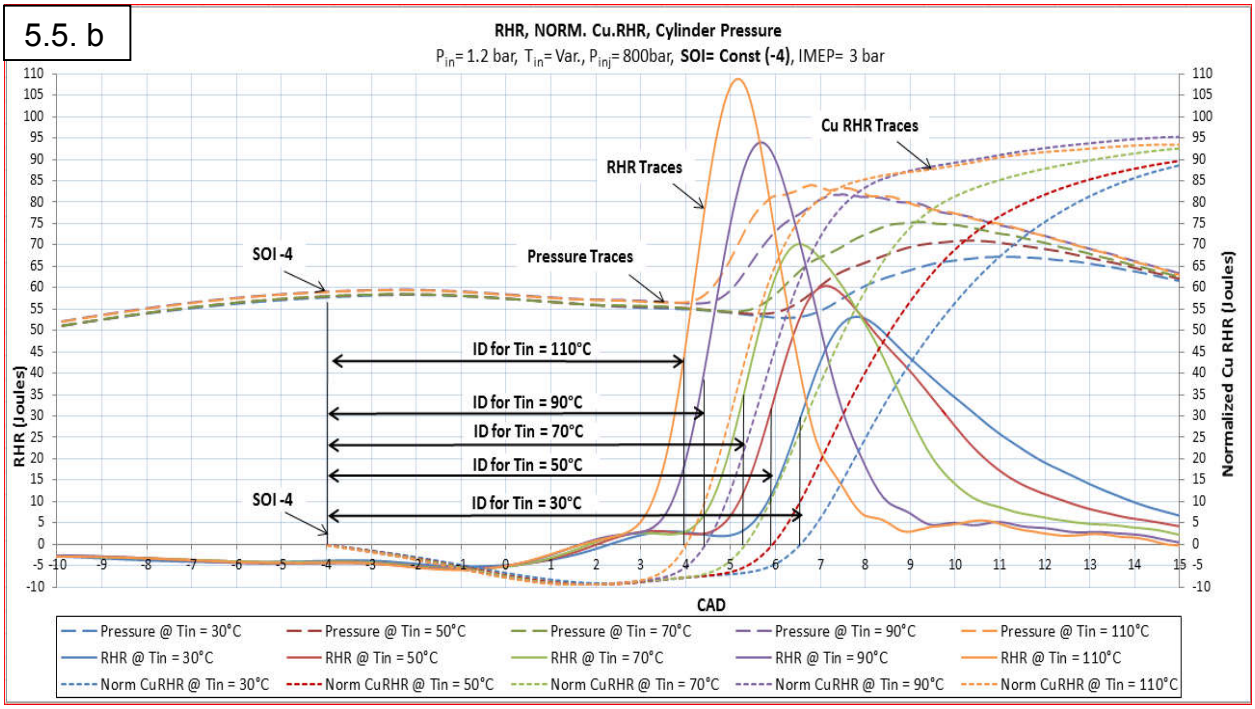

Figure 5.5.b : ID determination for SOI -4 with varying intake air temperature

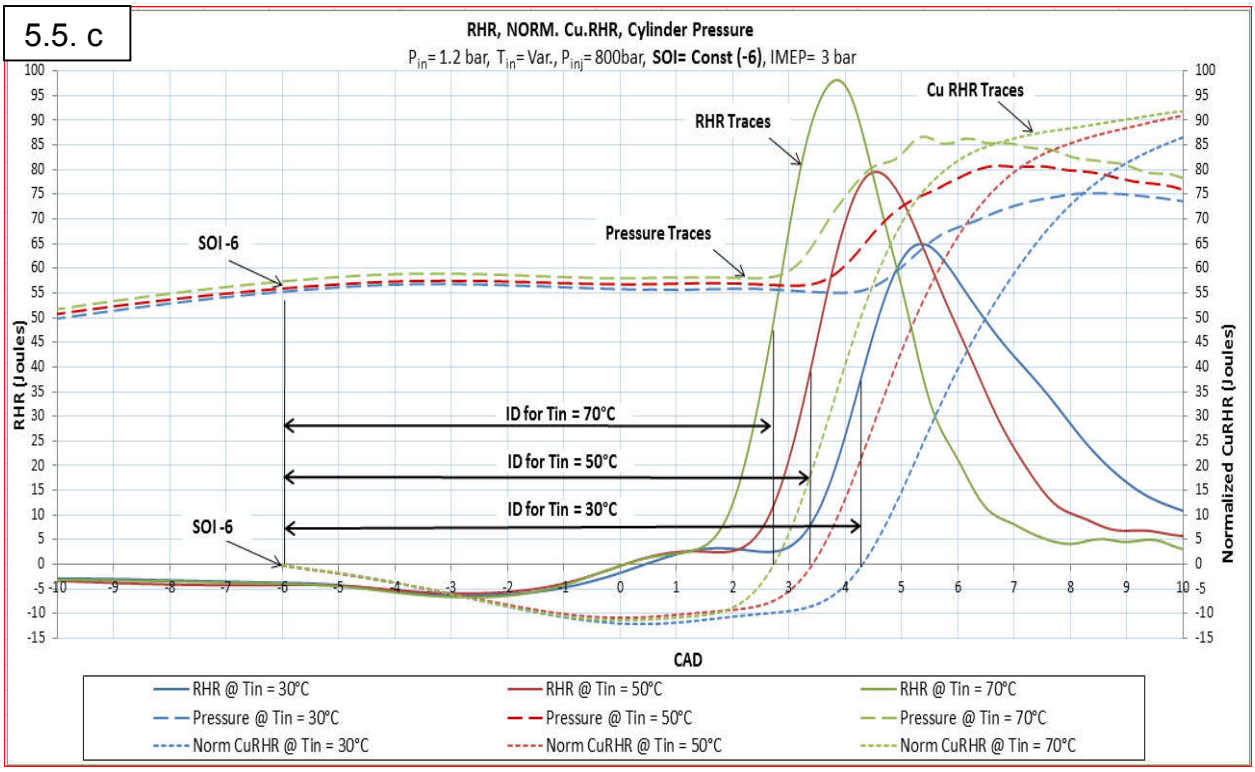

Figure 5.5.c : ID determination for SOI -6 with varying intake air temperature

	SOI (CAD)										
	-2			-4					-6		
Tin (°C)	70	90	110	30	50	70	90	110	30	50	70
ID (ms)	1.19	1.12	1.03	1.17	1.11	1.04	0.93	0.89	1.14	1.04	0.97
ID (CAD)	10.7	10.1	9.25	10.5	10	9.35	8.35	8	10.3	9.4	8.75

Table 5.3: ID values

Table 5.3 shows, ID values for the three SOI at varying intake air temperatures in tabulated form. It is observed that for each SOI a higher intake air temperature shortens ID period.

5.2. Effect of varying SOI at constant Intake Air Temperature

In this case, the intake air temperature is kept constant to show the effect of varying SOI on pressure, temperature, RHR and NTC regime. The intake temperature of 70°C is chosen because it is the only temperature that is common in all the three SOIs (-2, -4 and -6). Lower intake air temperatures at early injection timing produce peak cylinder pressures higher than allowed for safe engine operation.

5.2.1. Effect of varying SOI at Intake Air Temperature of 70°C on Cylinder Pressure.

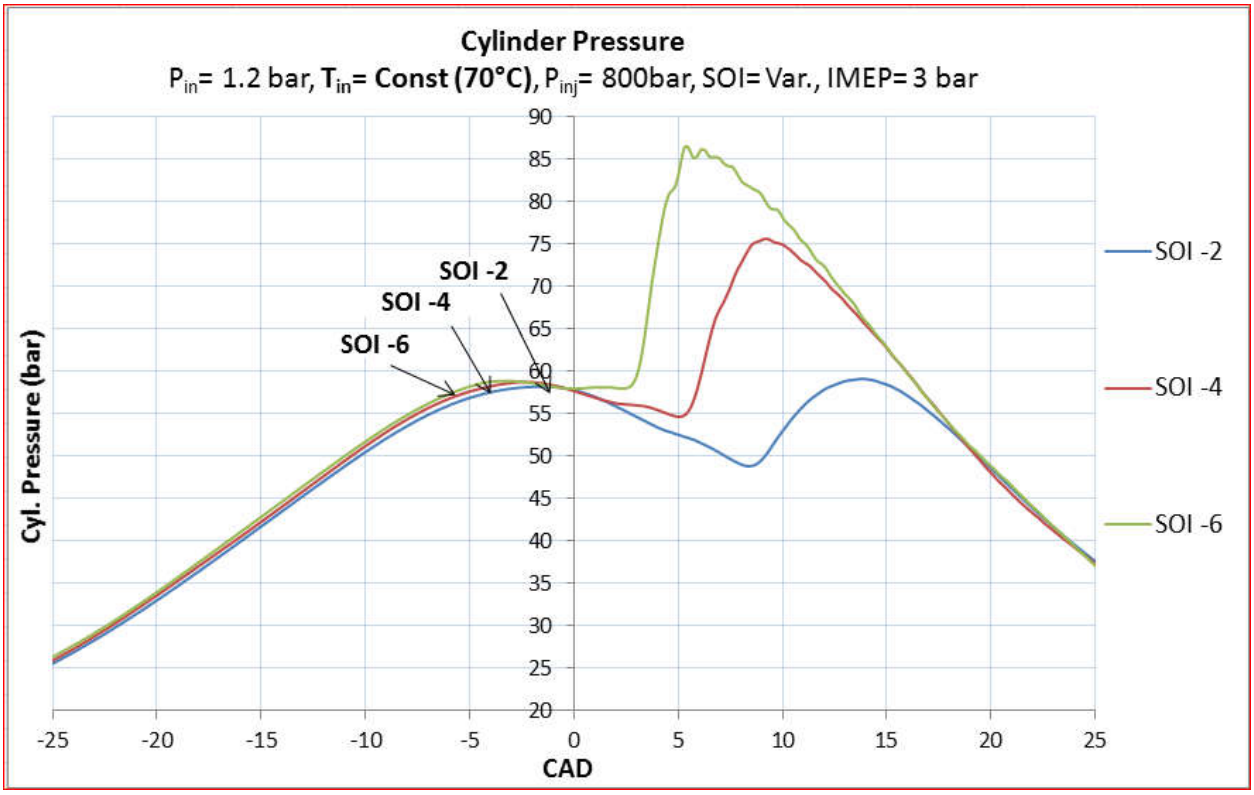

Figure 5.6: Pressure traces at constant T_{int} of 70°C and varying SOI of -2, -4, -6 CAD

Fig. 5.6 shows that at the same intake air temperature, the advanced SOI allows longer time for fuel evaporation at a charge temperature that is increasing due to compression before piston reaches TDC. Hence, at near TDC location where autoignition occurs, there is more homogenous mixture of air and fuel for better combustion. As SOI is advanced from -2 to -6, there is noticeable rise in peak pressure. Pressure rises from 58 bar to 87 bar with shift in location of peak pressure from 14 CAD to 5.5 CAD towards TDC.

5.2.2. Effect of varying SOI at Intake Air Temperature of 70°C on In-cylinder Temperature.

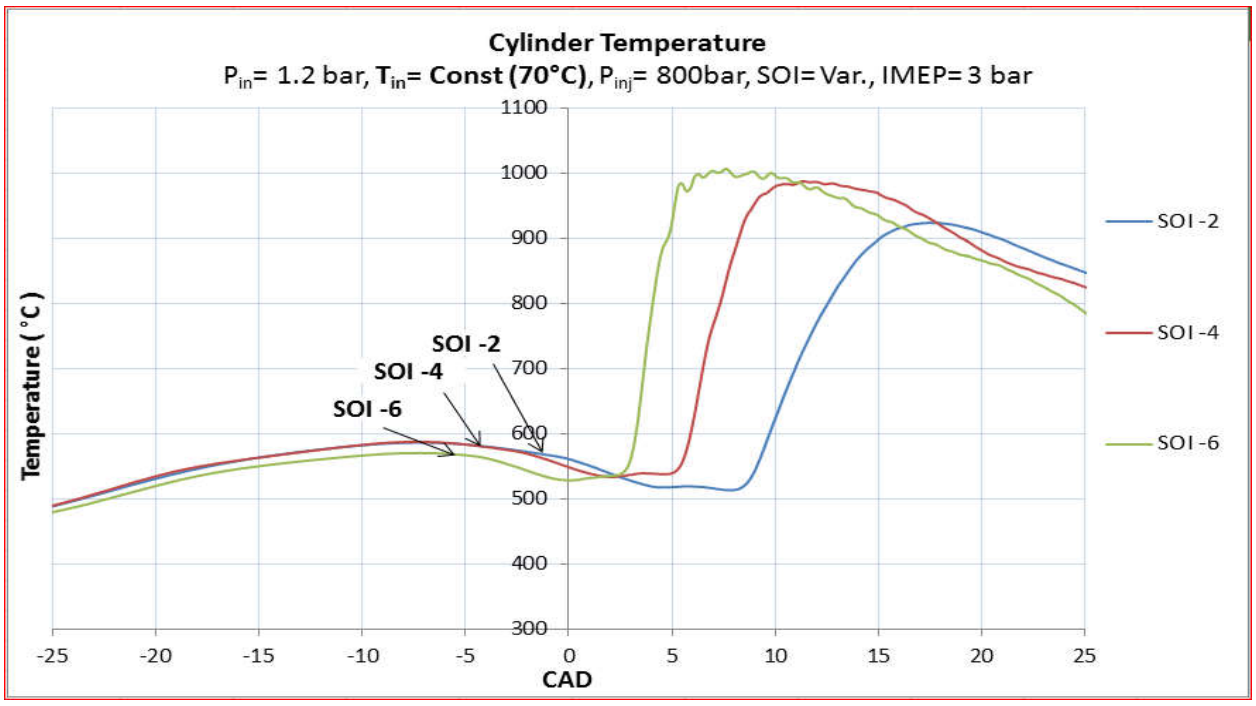

Figure 5.7: Temperature traces at constant T_{int} of 70°C and varying SOI of -2, -4, -6 CAD

Fig. 5.7 shows temperature traces generated for constant T_{int} of 70°C and SOIs of -2, -4 and -4 CAD. Temperature traces shows similar trend as in-cylinder pressure traces as explained earlier. As the SOI is advanced in-cylinder temperature increases from around 925°C to 1000°C and its peak shifts towards TDC. At more advanced SOI of -6, more cycle-to-cycle variation was observed.

5.2.3. Effect of varying SOI at Intake Air Temperature of 70ºC on Rate of Heat Release.

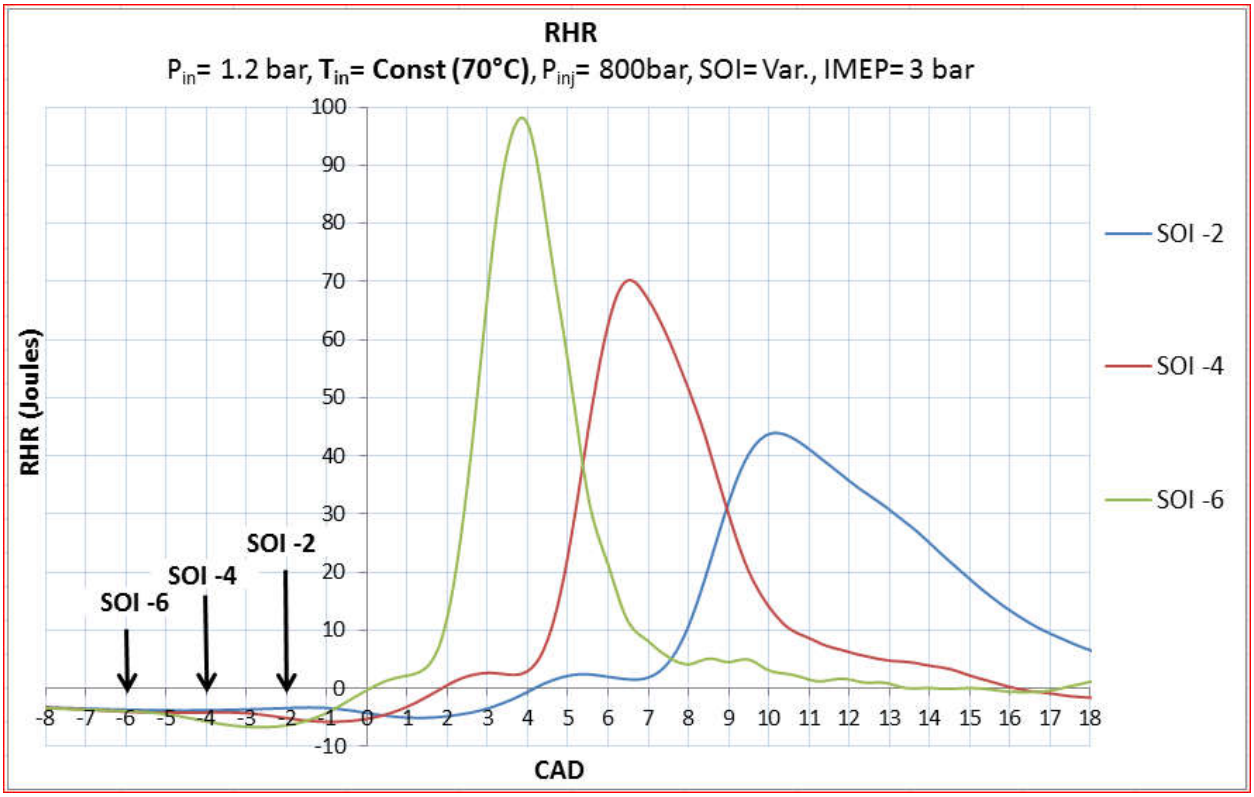

Figure 5.8: RHR traces at constant T_{int} of 70°C and varying SOI of -2, -4, -6 CAD

Fig. 5.8 shows the variation in RHR traces at constant intake air temperature and varying SOI. For the fuel injected at more advanced SOI, autoignition starts earlier, energy is released faster, producing higher peak of premixed combustion closer to TDC.

5.2.4. Effect of varying SOI at Intake Air Temperature of 70°C on NTC regime.

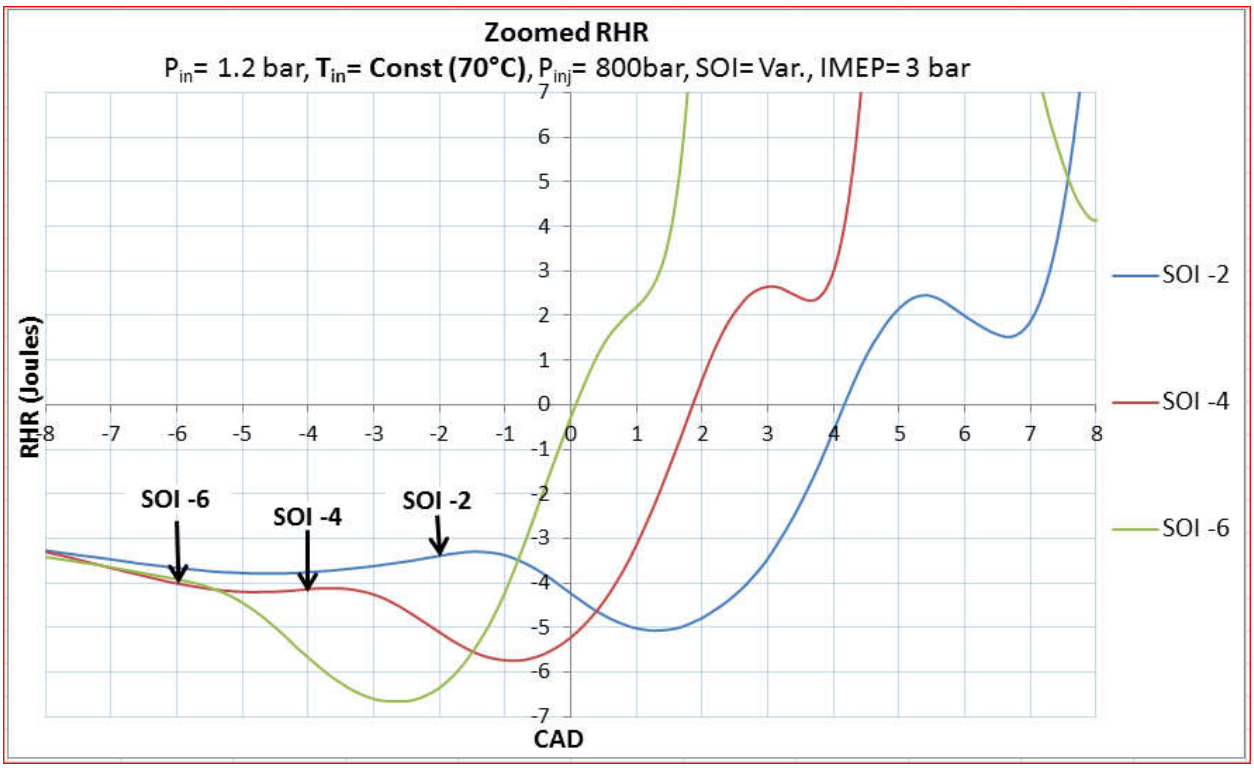

Figure 5.9: Zoomed RHR traces at constant T_{int} of 70°C and varying SOI of -2, -4, -6 CAD

Fig. 5.9, shows that advancing SOI reduces NTC regime and cool flame. When SOI is advanced from -2 to -4 CAD, duration of NTC regime decreased from around 1.5 CAD to 0.5 CAD. Further advancing SOI to -6 caused NTC regime to disappear leaving behind only small quantity of cool flame. This is the result of having the autoignitionn reaction completed during the compression stroke where the charge temperature continually increases due to compression.

5.2.5. Observations based on zoomed RHR graph

In this case, intake charge temperature is kept constant and SOI is advanced from -2 to -6. Observations are made for the lowest point in the RHR trace after SOI i.e.

the point where the exothermic reactions start to dominate over losses due fuel evaporation and endothermic reactions, causing an increase in charge temperature and pressure. Fig. 5.9 shows, as SOI is advanced from -2 to -4, there is drop in the value of RHR by approximately 1 joule. Similar drop is observed when SOI is advanced from -4 to -6. When SOI is advanced from -2 to -4, a phase shift of 2 CAD towards TDC is observed in the location of the lowest point in RHR trace after SOI. However, when SOI is advanced from -4 to -6, this shift is observed to be 1.5 CAD.

5.2.6. Ignition Delay Determination at varying SOI

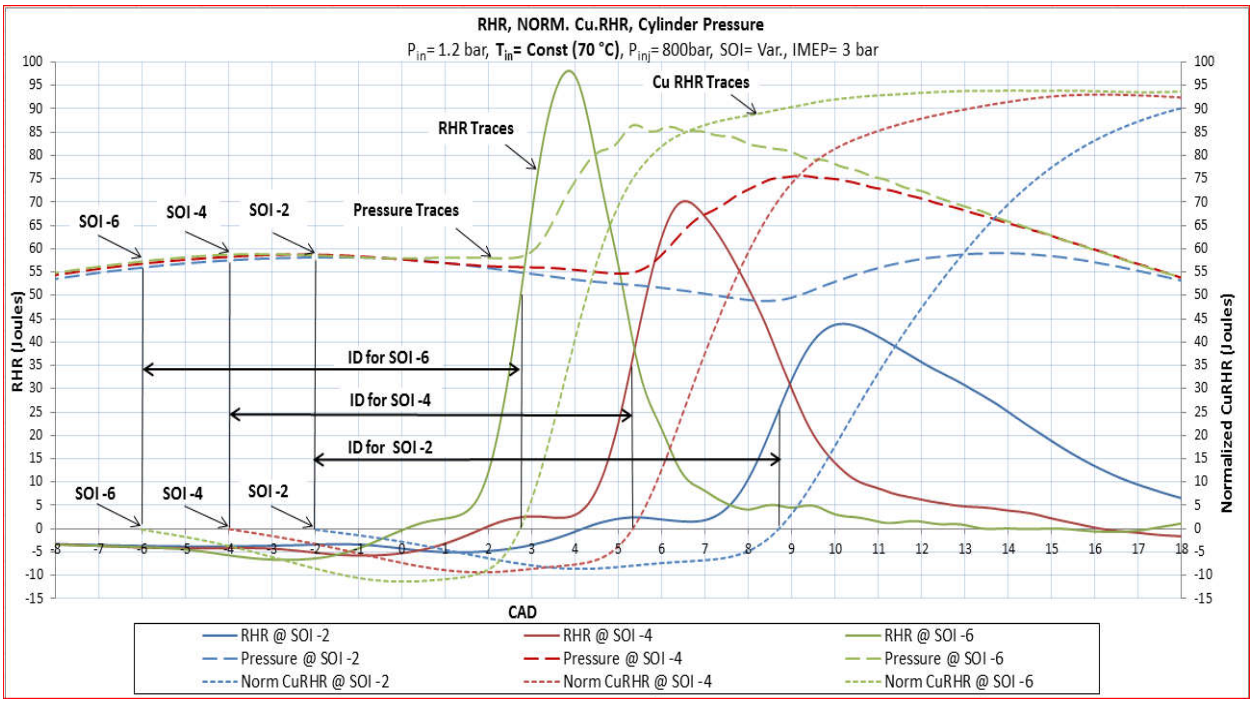

Figure 5.10: ID determination for SOI -2, -4, -6 at constant intake air temperature

Fig. 5.10. shows, the ignition delay determined at varying SOI and constant intake air temperature. For the constant T_{in} when SOI is advanced ID decreases, because fuel is injected early in compression stroke.

	SOI (CAD)		
	-2	-4	-6
Tin (°C)	70	70	70
ID (ms)	1.19	1.04	0.97
ID (CAD)	10.7	9.35	8.75

Table 5.4.: ID values for SOI -2, -4 and -6 at constant T_{in}.

Table 5.4 shows the ID for different SOIs at a constant T_{in}.of 70°C. Advancing SOI from -2 to -4, reduced ID by 12.6%. Advancing SOI from -2 to -6, ID reduced ID by 18.5%. The reason for this change in ID is explained earlier.

5.3. Activation Energy (Ea) calculations:

Activation Energy (Ea) is the incremental energy needed for the reacting species, in a simple elementary reaction, before they proceeds to form the final products. Since the autoignition reactions involve a huge number of elementary reactions, the activation energy calculated from the ignition delay and Arrhenius plot, is referred to as “Apparent Activation Energy for the Global Autoignition Reaction, E_a. E_a is simply referred to as the activation energy.

Arrhenius equation is used to calculate Ea values using ID of Sasol fuel. Arrhenius plots are plotted with natural log of ID values versus temperature inverse. Slope of the Arrhenius plots gives Ea/Ru values from which Ea is calculated.

Since ID is the time elapsed between SOI and SOC, attention is paid on deciding appropriate definition for SOC. Out of the available SOC definitions in the literature, two definitions which take into account the two stages of autoignition observed for the low cetane number Sasol fuels were compared. SOC at the point where 5% mass burn

fraction occurs (CA5), is compared with SOC at the point where CuRHR crosses zero. (CA_{RP}). 5 % mass burn fraction occurs at 5 % cumulative RHR.

Arrhenius plots for determination of activation energy using the two definitions of ID are plotted for Ea/Ru values. Data points used are same as given in Table 5.1.

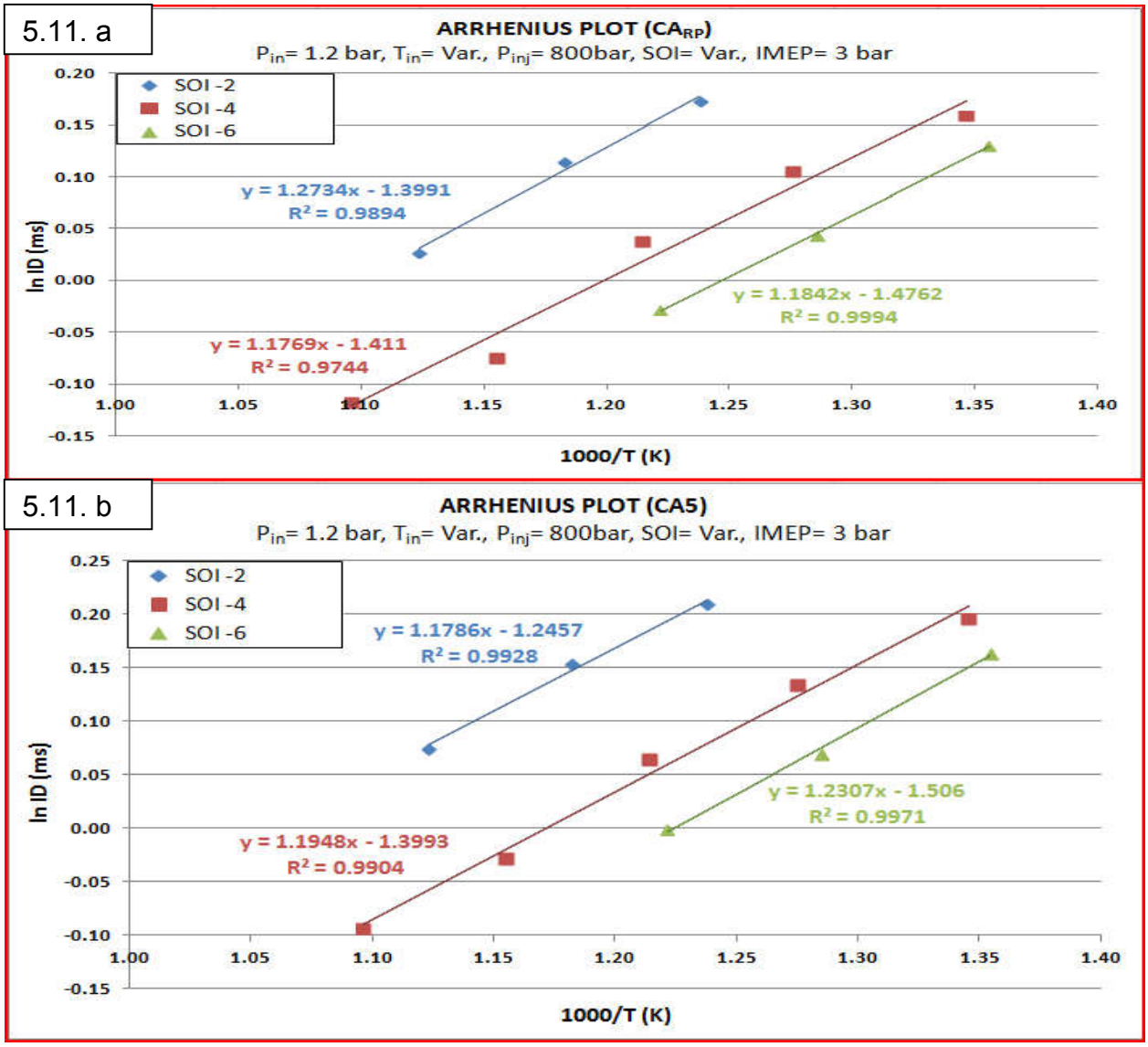

Figure 5.11: Arrhenius plots of ID v/s 1/T for CA_{RP} and CA5

In Fig. 5.10, ln ID is plotted versus 1000/T. The slope of the straight line gives E_a/Ru value from which activation energy for different injection timings is calculated.

Actual SOI	T_{in} (°C)	ID (CA_{RP}) CAD	ID (CA5) CAD	T_{mean} CA_{RP} (°C)	T_{mean} CA5 (°C)	Ea (KJ/kg mole) - CA_{RP}	Ea (KJ/kg mole) - CA5
-2	70	10.7	11.1	534.7	534.9	10587.05	9798.88
-2	90	10.1	10.5	572.8	573.0		
-2	110	9.3	9.7	617.1	617.3		
-4	30	10.6	10.95	469.8	470.3	9784.75	9933.57
-4	50	10.0	10.3	510.8	511.2		
-4	70	9.4	9.6	550.6	550.8		
-4	90	8.4	8.75	592.6	592.9		
-4	110	8.0	8.2	639.3	639.3		
-6	30	10.3	10.6	464.7	465.2	9845.44	10232.04
-6	50	9.4	9.65	505.1	505.5		
-6	70	8.8	9	545.5	545.7		

Table 5.5: Calculation of Ea for CA_{RP} and CA5 SOC definitions.

Table 5.5 and Figure 5.11 show the values obtained for the activation energy using two different SOC definitions. The average value for the activation energy is 10030.3 kJ/kg mole and the standard deviation is 60.

5.4. Discussions

1. To study the change in ID values at different SOI, one more parameter is speculated in addition to temperature as contributing factor, P_{mean} or P_{SOI}. P_{mean} is the pressure from SOI to SOC and P_{SOI} is the pressure at SOI. So the equation for ID is modified as

$$ID = \frac{Ae^{\frac{Ea}{Ru\,Tm}}}{P^n}$$

Where all the other parameters remains same as the previous equation used in the report for ID calculations and *P* is either P_{mean} or P_{SOI}.

However, from the values of P_{mean} and P_{SOI} at different SOI and intake charge temperatures as mentioned in Table 5.6, it is observed that for same temperature range, at different SOI, the variation in pressure values is not significant since it is less than 4%. So considering mean pressure will not make major change in ID values.

Hence the assumption that, pressure during the ID period contributes in change of ID values could not be justified and mean temperature is the only major contributing factor for change in ID values.

Actual SOI	Tin (°C)	P mean (bar)	P SOI (bar)
-2	70	54.17	58.19
	90	54.37	58.08
	110	55.42	58.67
-4	30	56.38	57.86
	50	56.77	58.14
	70	57.09	58.27
	90	58.45	59.34
	110	58.44	59.26
-6	30	55.98	55.24
	50	56.83	55.79
	70	58.31	57.35

Table 5.6: P_{mean} and P_{SOI} values at different intake temperature for particular SOI

Table 5.6. shows, values of mean Pressure and Pressure at different SOI at varying intake air temperature.

2. Negative Temperature Coefficient regime, in generic term, is represented by the drop in RHR trace due to aldehyde formation before start of combustion of fuel. This drop occurs after the exothermic reaction starts and RHR trace crosses zero to reach a point where aldehydes formed are high enough to reduce the heat

release rate. Higher the amount of aldehydes formed, more will be the drop in the RHR which will delay the start of combustion. As the rate of aldehyde oxidation increases, heat release rate increases marking start of combustion.

3. Advanced SOIs allow more fuel to evaporate during compression and increases premix combustion fraction and rate of combustion, as shown from increase in rate of heat release slopes during combustion.

CHAPTER 6

CONCLUSIONS AND RECOMMENDATIONS

6.1. Conclusions

These conclusions are based on an experimental investigation on the single-cylinder PNGV (Partnership of New Generation of Vehicles) to determine the autoignition characteristics of Sasol IPK (Iso Paraffinic Kerosene).

- Different definitions for the ID were investigated considering several parameters for the start of combustion. In this investigation the start of combustion is chosen to accounts for the two stage ignition common to low cetane number fuels such as Sasol..
- As intake air temperature is increased keeping SOI constant, ID decreased due to higher combustion temperature and pressure reached during the ID period.
- As SOI is advanced from -2 CAD to -6 CAD, at a constant intake air temperature of 70°C, ID decreased by 18%. Early injection timing allowed the autoignition reactions to be completed during the compression stroke where the gas temperature increased by compression.
- The autoignition of Sasol experienced the low temperature (cool flame) and NTC regimes at the relatively low gas temperatures which occurred in late start of injection and low inlet air temperatures. Earlier injection and higher intake air temperatures reduced the NTC regime. Both the low temperature and NTC regimes were eliminated at -6 CAD and inlet temperature of 70°C.

- In this investigation the change in the mean pressure during the ID was negligible and the charge temperature was the main parameter that had an impact on the ID period.
- The variation in the apparent activation energy for the global autoignition reactions of Sasol was negligible and an average value for Ea was found to be 10030.3 kJ/kg mole.

6.2. Recommendations

- Since Sasol low DCNT cannot replace JP8, this investigation should be extended to determine the autoignition characteristics of blends of JP8 and Sasol low CN fuel.
- Similar investigations should be conducted at low ambient temperatures which occur during cold starting of diesel engines. This is particularly important in heavy duty high power density turbocharged diesel engines.

APPENDIX A

Table A.1: Properties of Target Fuel (Sasol IPK)

Properties	**Sasol IPK**
Derived Cetane Number	31.17
Aromatic Content	0.2
Molecular Weight	158.8
H/C	2.27
Smoke Point	40.5
Density	0.745
Boiling Point	152.61-221.39°C
Lower Heating Value	44

APPENDIX B

TEST CONDITIONS	
Engine Speed	1500 rpm
Fuel Injection Pressure	800 bar
Swirl Ratio	3.77
IMEP	3 bar
Charge density	Constant
Oil Temperature	90 °C
Coolant Outlet Temperature	180 °C
TEST MATRIX	
CAD	Intake Charge Temperature° C
SOI -2	70
	90
	110
SOI -4	30
	50
	70
	90
	110
SOI -6	30
	50
	70

REFERENCES

[1] Harrison, W. "The role of Fischer Tropsch fuels for the US military." National Aerospace Fuels Research Complex. Air Force Research Laboratory, Wright-Patterson AFB, Ohio 30 (2006).

[2] Le Pera, M. E. "The reality of the single-fuel concept." Army logistician 37.2 (2005): 41-43.

[3] J. Heywood, "Internal Combustion Engine Fundamentals", McGraw Hill, New York, 1988.

[4] "Two-stroke Low Speed Diesel Engines for Independent Power Producers and Captive Power Plants," MAN Diesel, 2009.

[5] T. Takaishi, A. Numata, R. Nakano, and K. Sakaguchi, "Approach to High Efficiency Diesel and Gas Engines," Mitsubishi Heavy Industries Ltd., 2008.

[6] Kouremenos, D.A., D.T. Hountalas, and A.D. Kouremenos, "Experimental Investigation of the Effect of Fuel Composition on the Formation of Pollutants in Direct Injection Diesel Engines", DOI: 10.4271/1999-01-0189, SAE International, 1999.

[7] Zhong, L., N.A. Henein, and W. Bryzik, "Simulation-Based Cold-Start Control Strategy for a Diesel Engine with Common Rail Fuel System at Different Ambient Temperatures", DOI: 10.4271/2007-01-0933, SAE International, 2007.

[8] Benajes, J., et al., "The effect of swirl on combustion and exhaust emissions in heavy-duty diesel engines", 218(10): p. 1141-1148, Proceedings of the Institution of Mechanical Engineers, Part D: Journal of Automobile Engineering, 2004.

[9] Sun, Y. and R.D. Reitz, "Modeling Diesel Engine NOx and Soot Reduction with Optimized Two-Stage Combustion", DOI: 10.4271/2006-01-0027, SAE International, 2006.

[10] Kook, S., et al., "The Effect of Swirl Ratio and Fuel Injection Parameters on CO Emission and Fuel Conversion Efficiency for High-Dilution, Low-Temperature Combustion in an Automotive Diesel Engine", DOI: 10.4271/2006-01-0197, SAE International, 2006.

[11] Sun, Y. and R.D. Reitz, "Adaptive Injection Strategies (AIS) for Ultra-Low Emissions Diesel Engines", DOI: 10.4271/2008-01-0058, SAE International, 2008.

[12] Vishwanathan, G. and R.D. Reitz, "Numerical Predictions of Diesel Flame Lift-off Length and Soot Distributions under Low Temperature Combustion Conditions", DOI: 10.4271/2008-01-1331, SAE International, 2008.

[13] Tsujimura, T., M. Oguma, and S. Goto, "A Study of Fuel Auto-ignitability on Premixed Compression Ignition Characteristics", DOI: 10.4271/2008-01-0062, SAE International, 2008.

[14] Bruneaux, G., "Study of the Correlation Between Mixing and Auto-Ignition Processes in High Pressure Diesel Jets", DOI: 10.4271/2007-01-0650, SAE International, 2007.

[15] Yamashita, H., et al., "Research of the DI Diesel Spray Characteristics at High Temperature and High Pressure Ambient", DOI: 10.4271/2007-01-0665, SAE International, 2007.

[16] A. Sinha, C. Jayakumar, J. Nargunde, W. Bryzik, N. Henein, and K. Acharya, "Effect of Biodiesel and its Blends on Particulate Emissions from HSDI Diesel Engine," SAE Technical Paper 2010-01-0798, 2010.

[17] M. Dahodwala, V. Nagaraju, K. Acharya, W. Bryzik, and N. Henein, "Effect of Using Biodiesel (B-20) and Combustion Phasing on Combustion and Emissions in a HSDI Diesel Engine," SAE Technical Paper 2011-01-1203, 2011.

[18] J. Nargunde, "Auto-Ignition, Combustion And Emission Characteristics Of Soybean Biodiesel, Jet Propellant (jp-8) Fuel And Ultra Low Sulfur Diesel In A Single Cylinder Diesel Engine," MS, Wayne State University, Detroit, 2010.

[19] K. Zha, X. Yu, R. Florea, and M. Jansons, "Impact of Biodiesel Blends on In-cylinder Soot Temperature and Concentrations in a Small-Bore Optical Diesel Engine," SAE Technical Paper 2012-01-1311, 2012.

[20] B.-Q. He, J.-X. Wang, X.-G. Yan, X. Tian, and H. Chen, "Study on Combustion and Emission Characteristics of Diesel Engines Using Ethanol Blended Diesel Fuels," SAE Technical Paper 2003-01-0762, 2003.

[21] C. Kumar, M. Athawe, Y. V. Aghav, M. K. Gajendra Babu, and L. M. Das, "Effects of Ethanol Addition on Performance, Emission and Combustion of DI Diesel Engine Running at Different Injection Pressures," SAE Technical Paper 2007-01-0626, 2007, 2007.

[22] T. A. Nevius, D. Rauker, and S. T. Porter, "Investigation of Direct-Injected Ethanol and Diesel Fuel Blends on Gaseous and Particulate Emissions in a Medium-Duty Diesel Engine," SAE Technical Paper 2013-01-1141, 2013.

[23] K. Nord, D. Haupt, P. Ahlvik, and K.-E. Egebäck, "Particulate Emissions From an Ethanol Fueled Heavy-Duty Diesel Engine Equipped With EGR, Catalyst and DPF," SAE Technical Paper 2004-01-1987, 2004.

[24] S. H. Park, J. Cha, and C. S. Lee, "Impact of biodiesel in bioethanol blended diesel on the engine performance and emissions characteristics in compression ignition engine," Applied Energy, 99, pp. 334-343, 2012.

[25] C. Jayakumar, Z. Zheng, U. Joshi, W. Bryzik, N. Henein, and E. Sattler, "Effect of Intake Pressure and Temperature on the Auto-Ignition of Fuels with Different Cetane Number and Volatility," SAE Technical Paper 2012-01-1317, 2012.

[26] K. Wadumesthrige, N. Johnson, M. Winston-Galant, E. Sattler, N. Bezaire, S. Zeng, S. Salley, and K. Y. Ng, "Performance, Durability, and Stability of a Power Generator Fueled with ULSD, S-8, JP-8, and Biodiesel," SAE Technical Paper 2010-01-0636, 2010.

[27] R. M. George, T. Badawy, and N. Henein, "Experimental Study for the Effect of Fuel Properties on the Ion Current, Combustion, and Emission in a High Speed Diesel Engine," SAE Technical Paper 2014-01-1263, 2014.

[28] Z. Zheng, T. Badawy, N. Henein, E. Sattler, and N. Johnson, "Effect of Cetane Improver on Autoignition Characteristics of Low Cetane Sasol IPK Using Ignition Quality Tester (IQT)," J. Eng. Gas Turbines Power, 136(8), 2013.

[29] K. Zha, X. Yu, M.-C. Lai, and M. Jansons, "Investigation of Low-Temperature Combustion in an Optical Engine Fueled with Low Cetane Sasol JP-8 Fuel Using OH-PLIF and HCHO Chemiluminescence Imaging," SAE Technical Paper 2013-01-0898, 2013.

[30] S. Kook, and L. M. Pickett, "Soot Volume Fraction and Morphology of Conventional, Fischer-Tropsch, Coal-Derived, and Surrogate Fuel at Diesel Conditions," SAE Technical Paper 2012-01-0678, 2012.

[31] P. Schihl, L. Hoogterp-Decker, and E. Gingrich, "The Ignition Behavior of a Coal to Liquid Fischer-Tropsch Jet Fuel in a Military Relevant Single Cylinder Diesel Engine," SAE Technical Paper 2012-01-1197, 2012.

[32] N. A. Henein, and C.-S. Lee, “Autoignition and Combustion of Fuels In Diesel Engines Under Low Ambient Temperatures,” SAE International, 861230, 1986, DOI: 10.4271/861230.

[33] K. Acharya, M. Dahodwala, W. Bryzik *et al.*, “Effect of Different Biodiesel Blends on Autoignition, Combustion, Performance and Engine-Out Emissions in a Single Cylinder HSDI Diesel Engine,” SAE International, 2009-01-0489, 2009, DOI: 10.4271/2009-01-0489.

[34] H. J. Magdi K. Khair, “Combustion in Diesel Engines,” *DieselNet Technology*, 2010.

[35] R. Catalua, and R. da Silva, “Effect of Cetane Number on Specific Fuel Consumption and Particulate Matter and Unburned Hydrocarbon Emissions from Diesel Engines,” *Journal of Combustion,* vol. 2012, pp. 6, 2012.

[36] W. Yu, G. Chen, and H. Zuohua, “Influence of cetane number improver on performance and emissions of a common-rail diesel engine fueled with biodieselmethanol blend,” *Frontiers in Energy,* vol. 5, no. 4, pp. 412-418, 2011.

[37] V. Nagaraju, N. Henein, A. Quader *et al.*, “Effect of Biodiesel (B-20) on Performance and Emissions in a Single Cylinder HSDI Diesel Engine,” SAE International, 2008-01-1401, 2008, DOI: 10.4271/2008-01-1401.

[38] H. B. Dixon, L. Bradshaw, and C. Campbell, "Firing of gases by adiabatic compression. Part I. Photographic analysis of flame.," Journal of Chemical Society, Transactions, 55(2), pp. 2027-2035, 1914.

[39] C. J. Hawks, "Some experimental work in connection with diesel engine - fuel oil in diesel engines," Engineering, 110, pp. 127-131, 1920.

[40] A. Otto, "Combustion of Liquid Fuels in Diesel Engine", National Advisory Committee for Aeronautics Technical Memo, 1924.

[41] K. Neuman, "Experiments on Self Ignition of Liquid Fuels", National Advisory Committee for Aeronautics Technical Memo, 1926.

[42] F. Sass, "Ignition and Combustion Phenomena in Diesel Engines", National Advisory Committee for Aeronautics Technical Memo, 1928.

[43] J. Tausz, and F. Shulte, "Determination of ignition points of liquid fuels under pressure", National Advisory Committee for Aeronautics Techical Memo, 1925.

[44] J. Tausz, and F. Schulte, "Ignition Points and Combustion Reactions in Diesel Engines", National Advisory Committee for Aeronautics Technical Memo, 1928.

[45] J. Tausz, and F. Schulte, "Ignition Points and Combustion Reactions in Diesel Engines", National Advisory Committee for Aeronautics Technical Memo, 1928.

[46] A. M. Rothrock, "The NACA apparatus for studying the formation and combustion of fuel sprays and the results preliminary tests", National Advisory Committee for Aeronautics Report, 1932.

[47] A. M. Rothrock, and C. D. Waldron, "Fuel vaporization and its effect on combustion in a high speed CI engine", National Advisory Committee for Aeronautics Technical Notes, 1932.

[48] C. Miller, "Slow-motion Study of Injection and Combustion of Fuel In a Diesel Engine," SAE Technical Paper 450235, 1945.

[49] W. Wenzel, "Ignition Process in Diesel Engines," NACA Technical Memo No., 797, 1936.

[50] T. Yu, O. A. Uyehara, P. S. Myers, R. N. Collins, and K. Mahadevan, "Physical and Chmeical Ignition Delay in an Operating Diesel Engine Using the Hot-Motored Technique," SAE Technical Paper 560061, 1956.

[51] R. Hurn, J. Chase, C. Ellis, and K. Hughes, "Fuel Heat Gain and Release in Bomb Ignition," SAE Technical Paper 560062, 1956.

[52] El Wakil, M. Myers, P. S. Myers, and O. A. Oyehara, "Fuel Vaporization and Ignition Lag in Diesel Combustion," SAE Technical Paper 560063, 1956.

[53] W. T. Lyn, and E. Valdmanis, "The Effects of Physical Factors on Ignition Delay," SAE Technical Paper 680102, 1968.

[54] N. A. Henein, "A Mathematical Model for the Mass Transfer and Combustible Mixture Formation Around Fuel Droplets," SAE Technical Paper 710221, 1971.

[55] P. S. Pederson, and B. Quale, "A Model for the Physical Part of the Ignition Delay in a Diesel Engine," SAE Technical Papers 740716, 1974.

[56] T. W. R. III, "Correlation of Physical and Chemical Ignition Delay to Cetane Number," 1985.

[57] P. F. Flynn, R. P. Durrett, G. L. Hunter, A. O. z. Loye, O. C. Akinyemi, J. E. Dec, and C. K. Westbrook, "Diesel Combustion: An Integrated View Combining Laser Diagnostics, Chemical Kinetics, And Empirical Validation," SAE Technical Paper 1999-01-0509, 1999.

[58] J. Dec, "A Conceptual Model of DI Diesel Combustion Based on Laser-Sheet Imaging*," SAE Technical Paper 970873, 1997.

[59] W. Hwang, J. Dec, and M. Sjöberg, "Spectroscopic and chemical-kinetic analysis of the phases of HCCI autoignition and combustion for single- and two-stage ignition fuels," Combustion and Flame, 154(3), pp. 387-409,, 2008.

[60] J. Chen, T. Litzinger, and H. Curran, "The Lean Oxidation of Iso-Octane | at Elevated Pressures," SAE Technical Paper 2005-01-3734, 2005.

[61] C. K. Westbrook, "Chemical kinetics of hydrocarbon ignition in practical combustion systems," Proceedings of the Combustion Institute, 28(8), pp. 1563-1157, 2000.

[62] E. J. Silke, W. J. Pitz, C. K. Westbrook, M. Sjöberg, and J. E. Dec, "Understanding the Chemical Effects of Increased Boost Pressure under HCCI Conditions," SAE Int. J. Fuels Lubr. 1(1):12-25, 2009.

[63] K. Kuwahara, and H. Ando, "Role of Heat Accumulation by Reaction Loop Initiated by H2O2 Decomposition for Thermal Ignition," SAE International, 2007.

[64] G. D. Boerlage, and J. J. Broeze, "The Ignition Quality of Fuels in Compression Ignition Engines," Engineering, pp. 603-606, 687-689, 755-757, 1931.

[65] G. D. Boerlage, and J. J. Broeze, "Ignition Quality of Diesel Fuels as Expressed in Cetane Numbers," SAE Journal, 31, p. 283, 1932.

[66] H. H. Wolfer, "Ignition Lag in the Diesel Engine," VDI --- Forschumgshelft(392), 1938.

[67] F. A. F. Schmidt, "Theoretical and Experimental Study of Ignition Lag and Engine Knock", National Advisory Committee for Aeronautics Technical Memo, 1939.

[68] A. C. West, and D. Taylor, "Ignition Lag in a Supercharged C. I. Engine," Engineering, pp. 281-282., 1941.

[69] M. A. Elliott, "Combustion of Diesel Fuel," SAE Quarterly Trans., 3, pp. 490-515, 1949.

[70] R. Mueller, "Untersuchung des Verbrennungsvergangs deutscher Schwerole in einer Versuchsbombe , 1, 1936, pp. 1-10," Kraftfahretech, Forschungsarb. No. 3, pp. 1-10, 1936.

[71] W. Jost, "Explosion and Combustion Processes in Gases", McGraw Hill, New York, 1946.

[72] R. W. Hurn, J. O. Chase, C. F. Ellis *et al.*, “Fuel Heat Gain and Release in Bomb Ignition,” SAE Trans*,* vol. 64, pp. 703-711, 1956.

[73] T. C. Yu, R. N. Collins, K. Mahadevan *et al.*, “Physical and Chmeical Ignition Delay in an Operating Diesel Engine Using the Hot-Motored Technique,” SAE Trans., vol. 64, pp. 690-702, 1956.

[74] M. M. El Wakil, P. S. Myers, and O. A. Uyehara, “Fuel Vaporization and Ignition Lag in Diesel Combustion,” *SAE Trans.,* vol. 64, pp. 712-726, 1956.

[75] N. A. Henein, and J. A. Bolt, "Ignition Delay in Diesel Engines," SAE Technical Paper 670007, 1967.

[76] N. A. Henein, and J. A. Bolt, "Correlation of Air Charge Temperature and Ignition Delay for Several Fuels in a Diesel Engine," SAE Technical Paper 690262, 1969.

[77] Higgins, B., D. Siebers, and A. Aradi, "Diesel-Spray Ignition and Premixed-Burn Behavior", DOI: 10.4271/2000-01-0940, SAE International, 2000.

[78] Jansons, M., et al., "Experimental Investigation of Single and Two-Stage Ignition in a Diesel Engine", DOI: 10.4271/2008-01-1071, SAE International, 2008.

[79] Pickett, L.M., D.L. Siebers, and C.A. Idicheria, "Relationship Between Ignition Processes and the Lift-Off Length of Diesel Fuel Jets", DOI: 10.4271/2005-01-3843, SAE International,2005.

[80] Takada, K. and J. Kusaka, "Numerical Analysis of Diesel Combustion with High EGR and High Boost Pressure using a Multi-Dimensional CFD Code Coupled with Complex Chemistry Analysis", **1**(1): p. 1037-1048, SAE Int. J. Fuels Lubr., 2008.

[81] Jayakumar, Chandrasekharan, "Effect Of Intake Temperature And Boost Pressure On The Auto-Ignition Of Fuels With Different Cetane Numbers And Volatilities" (2013). Wayne State University Dissertations. Paper 772.

[82] Singh, Inderpal. Parametric analysis of combustion and engine-out emissions in a single cylinder HSDI diesel engine. Diss. WAYNE STATE UNIVERSITY, 2009.

[83] Joshi, Umashankar M., "Quantification Of Auto-Ignition In Diesel Engines" (2015). Wayne State University Dissertations. Paper 1341.

[84] A. J. Donkerbroek, M. D. Boot, C. C. M. Luijten, N. J. Dam, and J. J. ter Meulen, "Flame lift-off length and soot production of oxygenated fuels in relation with ignition delay in a DI heavy-duty diesel engine," Combustion and Flame, 158(3), pp. 525-538, 2011.

[85] R. P. Rodríguez, R. Sierens, and S. Verhelst, "Ignition delay in a palm oil and rapeseed oil biodiesel fuelled engine and predictive correlations for the ignition delay period," Fuel, 90(2), pp. 766-772, 2011.

[86] W. F. Colban, P. C. Miles, and S. Oh, "Effect of Intake Pressure on Performance and Emissions in an Automotive Diesel Engine Operating in Low Temperature Combustion Regimes," SAE Technical Paper 2007-01-4063, 2007.

[87] Y. V. Aghav, V. M. Thatte, M. N. Kumar, P. A. Lakshminarayanan, and M. K. G. Babu, "Predicting Ignition delay and HC emission for DI diesel engine encompassing EGR and Oxygenated fuels," SAE Technical Paper 2008-28-0050, 2008.

[88] D. B. Lata, and A. Misra, "Analysis of ignition delay period of a dual fuel diesel engine with hydrogen and LPG as secondary fuels," International Journal of Hydrogen Energy, 36(5), pp. 3746-3756, 2011.

[89] S. Kook, C. Bae, P. C. Miles, D. Choi, and L. M. Pickett, "The Influence of Charge Dilution and Injection Timing on Low-Temperature Diesel Combustion and Emissions," SAE Technical Paper 2005-01-3837, 2005.

[90] L. Murphy, and D. Rothamer, "Effects of Cetane Number on Jet Fuel Combustion in a Heavy-Duty Compression Ignition Engine at High Load," SAE Technical Paper 2011-01-0335, 2011.

[91] J. Cowart, M. Carr, P. Caton, L. Stoulig, D. Luning-Prak, A. Moore, and L. Hamilton, "High Cetane Fuel Combustion Performance in a Conventional Military Diesel Engine," SAE Technical Paper 2011-01-0334, 2011.

[92] D. Han, A. M. Ickes, S. V. Bohac, Z. Huang, and D. N. Assanis, "Premixed low-temperature combustion of blends of diesel and gasoline in a high speed compression ignition engine," Proceedings of the Combustion Institute, 33(2), pp. 3039-3046, 2011.

[93] A. Janssen, S. Pischinger, and M. Muether, "Potential of Cellulose-Derived Biofuels for Soot Free Diesel Combustion," SAE Int. J. Fuels Lubr., 3(1), pp. 70-84, 2010.

[94] C. Taylor, J. Baltrus, D. Driscoll, “Fisher Tropsch Fuels,” an article published in 2011 on US Department Of Energy, (http://www.netl.doe.gov/publications/factsheets/rd/R&D089.pdf).

[95] E. Frame, R. Alvarez, M. Blanks, Freerks *et al.*, “Alternative Fuels: Assessment of Fischer-Tropsch Fuel for Military Use in 6.5L Diesel Engine,” SAE Technical Paper, 2004-01-2961, 2004, DOI: 10.4271/2004-01-2961.

[96] L. L. Stavinoha, E. S. Alfaro, H. H. Dobbs *et al.*, “Alternative Fuels: Gas to Liquids as Potential 21st Century Truck Fuels,” SAE International, 2000-01-3422, 2000, DOI: 10.4271/2000-01-3422.

[97] P. Schihl, L. Hoogterp-Decker, and E. Gingrich, “The Ignition Behavior of a Coal to Liquid Fischer-Tropsch Jet Fuel in a Military Relevant Single Cylinder Diesel Engine,” *SAE Int. J. Fuels Lubr.,* vol. 5, no. 2, pp. 785-802, 2012.

[98] P. A. Muzzell, E. R. Sattler, A. Terry *et al.*, “Properties of Fischer-Tropsch (FT) Blends for Use in Military Equipment,” SAE International, 2006-01-0702, 2006, DOI: 10.4271/2006-01-0702. 209.

[99] C. A. Forest, and P. A. Muzzell, “Fischer-Tropsch Fuels: Why Are They of Interest to the United States Military?,” SAE International, 2005-01-1807, 2005, DOI: 10.4271/2005-01-1807.

[100] T. W. Chan, K. Cuddihy, W. Chishty *et al.*, “Gaseous and Particle Emissions from a Turbo-Jet Engine Operating on Alternative Fuels at Simulated Altitudes,” SAE International, 2011-01-2597, 2011, DOI: 10.4271/2011-01-2597.

[101] H. Wang, and M. A. Oehlschlaeger, “Autoignition studies of conventional and Fischer–Tropsch jet fuels,” *Fuel,* vol. 98, no. 0, pp. 249-258, 2012.

[102] P. W. Schaberg, I. S. Myburgh, J. J. Botha *et al.*, “Comparative Emissions Performance of Sasol Fischer-Tropsch Diesel Fuel in Current and Older 210 Technology Heavy-Duty Engines,” SAE International, 2000-01-1912, 2000, DOI: 10.4271/2000-01-1912.

[103] K. Wadumesthrige, N. Johnson, M. Winston-Galant *et al.*, “Performance, Durability, and Stability of a Power Generator Fueled with ULSD, S-8, JP-8, and Biodiesel,” SAE International, 2010-01-0636, 2010, DOI: 10.4271/2010-01-0636.

[104] S. Dooley, S. H. Won, S. Jahangirian *et al.*, “The combustion kinetics of a synthetic paraffinic jet aviation fuel and a fundamentally formulated, experimentally validated surrogate fuel,” *Combustion and Flame,* vol. 159, no. 10, pp. 3014-3020, 2012.

[105] X. Hui, K. Kumar, C.-J. Sung *et al.*, “Experimental studies on the combustion characteristics of alternative jet fuels,” *Fuel,* vol. 98, no. 0, pp. 176-182, 2012.

ABSTRACT

AN EXPERIMENTAL INVESTIGATION ON THE EFFECT OF INTAKE CHARGE TEMPERATURE AND INJECTION TIMING ON AUTOIGNITION OF LOW CETANE NUMBER FUEL (SASOL IPK)

by

SWAPNIL S BODELE

May 2016

Advisor: Dr. Naeim Henein

Major: Mechanical Engineering

Degree: Master of Science

Although diesel engines are considered best powerhouses for their heavy-duty capabilities, concerns are raised because of their emission issues and. Alternative fuels like jet fuels can be substitute to them with improved efficiencies. Department Of Defense uses JP8 for their combat vehicles under their Single Fuel Concept for better logistic supply chain. But, due to projected age of depletion of crude oil reservoirs, synthetic blends are being considered for their abundant availability.

One such blend, SASOL IPK, a Coal to Liquid based fuel prepared by Fisher-Tropsch process is considered in this study. This thesis shows results from experiments conducted on single cylinder PNGV engine to study the effect of intake charge temperature and injection timing on ignition delay of SASOL IPK. Speed, fuel injection pressure, swirl ratio and charge density were kept constant for all data points.

Two cases were considered, one with constant SOI and varying intake air temperature and other with constant intake air temperature and varying SOI. It was

observed that with increase in intake air temperature and advancing injection timing, ignition delay of the fuel reduced significantly. NTC regime and cool flame also decreased drastically at higher intake air temperatures and advanced injection timing.

ABBREVIATIONS

- PNGV – Program for New Generation of Vehicles
- T_{int} – Intake air temperature
- P_{inj} – Fuel Injection Pressure
- RHR – Rate of Heat Release
- CuRHR – Cumulative Rate of Heat Release
- DCN – Derived Cetane Number
- ID – Ignition Dealy
- SOI – Start Of Injection
- SOC – Start Of Combustion
- HCN – High Cetane Number
- LCN – Low Cetane Number
- E_a – Activation energy
- NTC – Negative Temperature Coefficient
- T_{mean} – Mean Temperature from SOI to SOC
- P_{mean} – Mean pressure from SOI to SOC
- P_{SOI} – Pressure at SOI

AUTOBIOGRAPHICAL STATEMENT

I remember walking down the road as a child and seeing all the cars around. Since that time, I was fascinated about auto sector and the powerhouse behind it. Today I feel moving closer towards the field I liked since that time.

I was born on 18 December 1986 in Mumbai, the City of Dreams as they call it. Through my father, I learned the importance of science in life and his motivation and my liking drove me towards the engineering field. I completed my bachelors in Mechanical Engineering in 2009 and started working in company manufacturing pressure vessels. During my job of three years, I realized that working in automotive industry is being missed in my life, so to study more about automobiles, especially engines I applied for Master's Degree program in Wayne State University. I joined PNGV lab in Center Of Automotive Research (CAR) group of the university under Dr. Henein. Working in the lab gave me an unmatched exposure to the instrumentation and equipments used for engine testing. Knowledge sharing sessions with lab and CAR team members taught me many new things. It has been the best phase of my life.

I believe, at the end things turnout to be good, working towards them is more important. Give your best, you will get the rest.